Theory of Crystallization under Equilibrium Polymerization in a Solution and the Investigation of Its Melting Properties

Sagar S. Rane[†,§] and P. D. Gujrati[*,†,‡]

Department of Polymer Science and Department of Physics, The University of Akron, Akron, Ohio 44325

Received November 17, 2004; Revised Manuscript Received July 25, 2005

ABSTRACT: We generalize a recently investigated lattice model of polydisperse semiflexible linear polymers formed under equilibrium polymerization in a solution [Gujrati, P. D.; Rane, S. S.; Corsi, A. *Phys. Rev. E* **2003**, *67*, 052501] and conduct a comprehensive investigation of its melting properties. Each polymer has two end groups and at least one chemical bond. The model is characterized by six energies, three of which are for the interaction between the middle group, the end group, and the solvent, and the remaining three represent conformational energies for a gauche bond, a hairpin turn, and a pair of neighboring parallel bonds. Two activities control the end group and the middle group densities and give rise to polydisperse chains whose chain lengths and numbers are not fixed. We study the melting properties such as the melting temperature, the latent heat, and the energy and entropy of fusion at fixed pressure as a function of various model parameters such as the monomer interactions, nature of end groups, chain rigidity, solvent quality, and degree of polymerization. Our theory is thermodynamically consistent in the entire parameter space and improves upon the classical theories; hence, our results should prove useful.

I. Introduction

The technological importance and the complexity of modeling polymer crystallization have drawn the interest of several scientists,[1−25] where the interest has been to study equilibrium melting. Most researchers have studied the original Flory model of melting[2] on a lattice because of its simplicity. Therefore, we will also consider a lattice model of melting in this work. Flory[2] had argued that the semflexibility is the most important factor in determining melting to be a first-order transition and that inter- and intramolecular interactions do not play an important role. However, it has also become clear[4,19−21] that to have first-order melting, in addition to the semiflexibility, the intermolecular interactions should also be in the correct physical range. Thus, the understanding of equilibrium melting is not complete at this moment. Experimental investigation of melting of macromolecules is complicated because the free energy barrier between the kinetically selected crystalline state and the true equilibrium state is so large that the kinetically selected metastable crystal state persists over time scales much longer than the experimental time scale.[17] It is also clear that nonequilibrium features *cannot* be understood well without a comprehensive understanding of equilibrium melting, which is far from complete. Therefore, this work is limited to investigating equilibrium melting only.

In this paper, we study the crystallization of linear chains (on a lattice) produced under the condition of equilibrium polymerization in a solution. Here, polymers can break anywhere along their backbone sequence, including the ends, and recombine at their ends reversibly in such a way that they maintain a particular equilibrium distribution of their lengths.[26] Even the number of chains is not fixed. Thus, one deals with a specific polydispersity in the chain length distribution and the number distribution. This should be contrasted with the conditions under which living polymers are formed, where polymers grow stepwise only at their ends under conditions that need not reach equilibrium.[27] The number of polymers remains fixed during living polymerization, whereas it is not fixed during equilibrium polymerization, though its average is. Thus, living polymerization is in equilibrium with respect to chemical bonds but not with respect to the number of polymers. Despite the differences, many authors treat living polymerization as equilibrium polymerization[14,27,28] as defined above. This issue has been discussed carefully in ref 29, to which we direct the reader. We will, henceforth, not make this association and distinguish between living and equilibrium polymerizations in this work. Examples of some systems that follow equilibrium polymerization, and which have been studied experimentally, include sulfur,[30] selenium,[31] ϵ-caprolactum,[32] laurolactum,[33] protein filaments[34] (e.g., actin, tubulin, flagellin, and fibrin), and systems of long wormlike micelles, e.g., cetyltrimethylammonium bromide/KBr/H_2O.[28b]

Equilibrium polymerization of athermal linear polymers has been widely studied[35,36] due to its deep connection with the $n = 0$ limit of an n-vector isotropic magnetic model. We will closely follow the connection developed in ref 36, where the weight of a solvent molecule is independent of the magnetic field H in the magnetic system. According to the magnetic analogy, there are only two activities that describe the polymer system. These activities are related to the ferromagnetic coupling strength J and the external magnetic field h. It is found that the activity κ for a chemical bond in a polymer and the activity of an end point η are given by[36]

$$\kappa = K/z, \quad \eta = H/\sqrt{z}$$

where $K = \beta J$, $H = \beta h$, $z = 1 + H^2/2$ and β is the inverse temperature in the units of the Boltzmann constant. The

* Corresponding author. E-mail: pdg@arjun.physics.uakron.edu.
† Department of Polymer Science.
‡ Department of Physics.
§ Present address: Department of Pharmaceutical Sciences, A317 ASTECC Building, University of Kentucky, Lexington, KY 40506-0286.

10.1021/ma047622f CCC: $30.25
Published on Web 09/21/2005

activities κ and η or the corresponding two chemical potentials describe an athermal polymer solution and control only the monomer and number densities (per lattice sites) ϕ_m and ϕ_p, so that the resulting solution is polydisperse. However, the particular polymer polydispersity is not fixed; it varies as the system's thermodynamic conditions change. The polydispersity is described uniquely by the number density distribution per lattice site $\phi_p(\ell)$ of chains of length $\ell = 1, 2, 3, \ldots$, which eventually determines the monomer density ϕ_m and the number density per lattice site ϕ_p via

$$\phi_m \equiv \sum_{\ell=1}^{\infty} \ell \phi_p(\ell) \quad \text{and} \quad \phi_p \equiv \sum_{\ell=1}^{\infty} \phi_p(\ell) \tag{1.1}$$

The average polymer length, called the degree of polymerization, is

$$M \equiv \phi_m/\phi_p \tag{1.2}$$

While the distribution $\phi_p(\ell)$ uniquely determines ϕ_m and ϕ_p, the converse is also true; i.e., the specification of ϕ_m and ϕ_p uniquely determines the polydispersity distribution $\phi_p(\ell)$. Thus, while it is possible that there are many different distributions that each have the same mean ϕ_p and the first moment ϕ_m, only a particular distribution is selected out of them as the equilibrium polydispersity distribution.

The thermodynamic state of the system in equilibrium polymerization is determined either by specifying the particular $\{\phi_p(\ell)\}$ mentioned above or by specifying ϕ_m and ϕ_p corresponding to the two chemical potentials. One can equivalently describe it by specifying M and ϕ_p. This requires choosing a particular path Γ_M in the space of the two chemical potentials along which M remains fixed. Only one chemical potential or activity is required to specify the polydisperse polymer system along Γ_M; this activity can be taken to control ϕ_p. It is obvious that the thermodynamic description along Γ_M is quite useful in that it allows us to compare this particular polydisperse system with a monodisperse system containing chains of a single length equal to M. The latter is a single-component system, in which a single chemical potential will control the density, such as ϕ_p. The monomer density in both systems is then determined uniquely by $\phi_m = M\phi_p$. The monodisperse system described by M and ϕ_p is similar to our above-mentioned variable polydisperse system along Γ_M. Throughout this work, this equivalence between the two systems will play a dominant role in our understanding of the processes that go on in the polydisperse system. For example, we expect only one melting transition in the monodisperse system. As we will see here, this is also true of the equilibrium polydisperse system.

Cautionary Note. If we consider changing the temperature, keeping constant the (lattice) volume, $\{\phi_p(\ell)\}$ will usually change in the polydisperse system. As a consequence, ϕ_p, ϕ_m, and therefore M will also change. In other words, the number density distribution $\{\phi_p(\ell)\}$ does not remain constant but continues to vary with temperature, keeping the volume fixed. In the following, we will call this equilibrium polydispersity variable polydispersity (and call it system A, whose specification requires two chemical potentials) to distinguish it from fixed polydispersity, in which $\{\phi_p(\ell)\}$ remains fixed under a constant volume temperature change, since the number of chains of a given length ℓ remains fixed in this system. We call the latter system B, whose specification requires as many chemical potentials as is the number of different allowed lengths in the system; it is actually a multicomponent system in which each $\phi_p(\ell)$ is controlled by its own chemical potential.

It is important for the reader to not confuse the two systems. The polydispersity in system B can be varied at will by adjusting the distribution of chains; there is no unique polydispersity for a given ϕ_p and ϕ_m. (Let us assume a constant volume in the following discussion, for simplicity.) However, once the polydispersity has been prescribed, the average chain length is fixed; it can no longer be changed as we change, for example, the temperature. The average chain length M in system A is not fixed, except along Γ_M on which system A acts like a single-component system like a monodisperse system. Because of the difference in the number of components, the phase diagram for the two systems A and B would be in general very different; see, for example, ref 24b. In particular, as we will see here, there is exactly one melting point in system A—the temperature where the free energy of the liquid phase matches the free energy of the crystal phase. This is the melting point that we report in this paper. On the other hand, there may be many different melting temperatures in system B. In this regard, system A is like a monodisperse system, and both will exhibit discontinuities in ϕ_p and ϕ_m. (However, we will see that there is a difference in that M in the two coexisting phases are different in system A but not in the monodisperse system due to variable polydispersity in system A.)

The magnetic mapping is also extended to the polymerization model of randomly branched athermal polymers of "even" functionality.[37] Following this connection, a thorough understanding of equilibrium polymerization of linear chains and branched polymers in athermal solutions has developed over the years, either with the use of the $n = 0$ limit[35−38] or without it.[28,39−48] The latter approach also allows consideration of polymer interactions. Equilibrium polymerization of (interacting) branched polymers also describe thermoreversible gelation and have been studied extensively by many authors.[41,43−51] However, all these studies are related to completely flexible polymers.

The study of crystallization, which requires semiflexibility, in linear chains under equilibrium polymerization has so far received little attention, though some important attempts have been made.[13−15,21,23−25] Most of the work is either numerical or phenomenological; in the latter case, the work is based on the random mixing approximation (RMA) used in the Flory theory.[2] However, not much information is available on how the melting properties of such polymers relate to the molecular parameters. Our goal in this paper is to fill in this gap by developing a theory for crystallization under equilibrium polymerization in a solution that goes beyond the RMA used in the classical Flory theory of melting[2] and conducting a comprehensive study of the melting properties. Our theory, in a sense, is also mean field in that it will predict classical values of critical exponents. However, as it goes beyond the RMA, it gives better results than the Flory theory in a quantitative sense, as has been demonstrated elsewhere.[52] The model we use here is an extension of the model proposed recently;[19,20] the extended model has already been used to study the role of free volume on the ideal glass transition in ref 21.

(a) Flory Model. The first derivation of lattice statistics in a model of semiflexible polymers with the mean field approximation was given by Flory,[1,2] where monodisperse polymers were considered. Flory has suggested that melting is mainly dictated by the semiflexibility and the excluded-volume interaction, and chain rigidity and intermolecular interactions can be neglected. This suggestion has been criticized[4] from the results of the exactly solvable models such as the KDP, F, and dimer models by mapping them onto polymer models; see also refs 8 and 16. Huggins obtained a better estimate for the probability of monomer insertion, which was shown to give more reliable[4,6] results for the melting temperature than the original Flory calculation. In a significant development, the results of Flory's theory were shown to be wrong, not just quantitatively but more important qualitatively by Gujrati and Goldstein.[5−7] We refer the reader to refs 6, 8, and 20 for further details. In particular, it was shown that no low-temperature inactive phase with perfect order can exist at nonzero temperatures ($T > 0$) in the Flory model because of the presence of the Gujrati−Goldstein excitations[5−8] involving hairpin turns, and the density of gauche bonds goes to zero only at $T = 0$. In an exact calculation on a Husimi cactus, which looks identical to a square lattice locally, it has been found that the melting transition in the Flory model is a tricritical point.[19,20] By introducing inter- and intramolecular interactions, we can obtain a first-order melting,[19−21] suggesting strongly that the inter- and intramolecular interactions may be very important in determining the order of the transition and, hence, must be accounted for.[4,8]

(b) Variable Polydispersity (Equilibrium Polymerization). The equilibrium polymerization is best described by a partition function requiring two chemical potentials, as discussed above. Such a partition function for the general polydisperse model of linear chains is presented in ref 20 (see eq 9b there) where we allow for semiflexibility, inter- and intramolecular interactions, polydispersity (controlled by the end group activity), and solvent or free volume. No distinction is made between the functional end groups and the middle groups of polymers. However, depending upon the functional groups used in initiation and termination, the end groups may be similar or very different from the middle groups. The importance of accounting for end group effects was recently demonstrated by us.[53] Therefore, we will extend the above model[20] to incorporate the difference between the end groups and the middle groups. The model is fully defined in the next section and has been used in ref 21 in a different context of investigating metastability and the ideal glass transition. Here, our interest is to only investigate the melting properties. We consider a square lattice so as to mimic a tetrahedral lattice needed to describe polymer crystals.

(c) Cactus Approximation. The model cannot be solved exactly. Hence, we make a single approximation, after which we solve the model exactly: We replace the original square lattice with a Husimi cactus,[19] which locally looks similar to the square lattice as both contain a simple square as the basic unit (see Figure 1). The squares are connected in a treelike fashion on the cactus, which makes the cactus different from the square lattice. The tree nature of the cactus allows us to solve the model exactly. The resulting solution is taken as an approximate theory for the original square lattice. The use of the Husimi cactus allows us to incorporate Gujrati−Goldstein excitations[5−8,19−21] that are responsible for destroying the completely ordered crystal phase in the Flory model. Thus, our theory is an improvement over the Flory theory. A general Husimi cactus made of ℓ-sided polygons ($\ell = 4$ for squares) also takes into account more correlations than the Bethe lattice[52] (another recursive lattice) due to the finite loop size. The Huggins approximation has been shown[4] to be exact on the Bethe lattice for a fully packed system. The Flory approximation for the probability of monomer insertion is also exact in the limit of the coordination number $q \to \infty$.[4] The Husimi cactus turns into the Bethe lattice as the loop size $\ell \to \infty$.[54] Thus, we also expect our theory to give better results than the Huggins approximation. Our method of solution is to use recursion relation technique proposed elsewhere.[52] We identify the crystalline state by a novel two-cycle fixed point scheme, which has been presented earlier.[19−21] The perfectly ordered crystalline state at absolute zero in the present theoretical treatment is of infinite size and consists of parallel arrangement of chains. At this time, we do not consider finite size crystallites or any particular type of unit cell or structure for the polymer; this is similar to the approach used by Flory.[2]

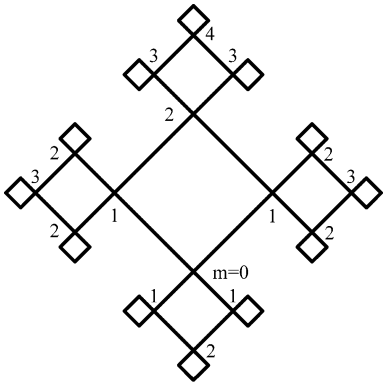

Figure 1. Husimi cactus and various levels. The level m increases as we move away from the origin $m = 0$. The numbers denote the indexing used for the crystalline phase. If the bottom vertex of a square is of level m, the two intermediate vertexes are of level $(m + 1)$ and the top vertex is of level $(m + 2)$. Even- and odd-numbered sites are labeled as two separate kinds of sites, A or B.

In the next two sections, we introduce the model and present the theory we shall use for our study. In section IV, we present our results for the melting properties. The last section contains the conclusions and a brief summary of our results. In the Appendix, we present the recursion relations and other equations used in the calculations.

II. Model

We consider a system consisting of solvent molecules and polydisperse linear polymers, which we take for simplicity to be defined on a square lattice of N sites. The end groups are treated as a different species from the middle groups. We will use monomers to collectively denote the middle and the end groups. Each monomer or solvent molecule occupies a site of the lattice. All lattice sites are occupied. Thus, we consider an incompressible polymer solution. It is also possible to think of the solvent molecules as representing voids. In that case, what we have is a compressible pure polymer system of variable polydispersity. The excluded-volume

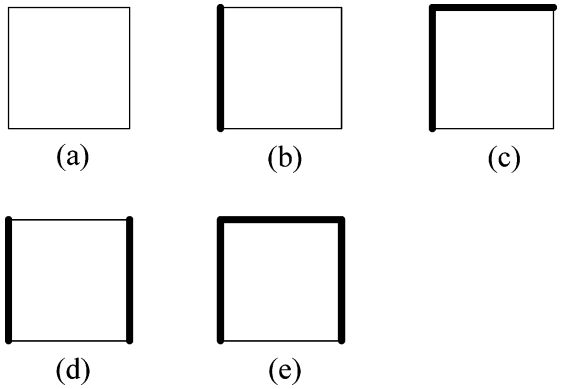

Figure 2. Five distinct states in a square cell: (a) $\sigma = 0$, no polymer bond; (b) $\sigma = 1$, two neighboring sites occupied by one bond; (c) $\sigma =$ g, two neighboring bonds making a bend; (d) $\sigma =$ p, two parallel bonds; (e) $\sigma =$ h, three bonds forming a hairpin turn.

effects are accounted for by imposing the requirement that only one monomer or solvent molecule can occupy a site of the lattice. We only allow nonbonded interactions between nearest-neighbor sites occupied by unlike species; this gives rise to the exchange energy in the system. In addition, there is the configurational energy between monomers. Three consecutive monomers on a polymer either are collinear or make a bend. To distinguish between the two possibilities, we allow a bending penalty $\epsilon > 0$ corresponding to a gauche bond. Four consecutive monomers on a polymer either make a single bend (that is controlled by the bending penalty above and does not require any additional control) or make two consecutive bends. The latter can give rise to two bends within the same square (hairpin turn) or in different squares (jagged turn). To distinguish between the two cases, we allow for an additional energy ϵ'' for a hairpin turn. Four monomers (belonging to the square) and not connected by consecutive bonds can either have no bond, one bond, or two bonds belonging to the square. Since the first two possibilities are not important for crystallization, we associate an additional energy ϵ' for the last possibility, in which the two bonds must be parallel.

We do not allow the possibility of any loop formation in the model, which makes our model different from those considered by, for example, Pandit and co-workers.[15]

Let us now consider the possible states of the four sites that belong to a square cell of the lattice. There are five distinct states σ that we need to consider, as shown in Figure 2: (a) $\sigma = 0$: There is no polymer bond inside the cell. (b) $\sigma = 1$: Two neighboring sites are occupied by one polymer bond. (c) $\sigma =$ g: Two polymer bonds requiring three sites are connected to each other, making a bend. (d) $\sigma =$ p: Two polymer bonds, each requiring two sites, are parallel to each other. (e) $\sigma =$ h: Three polymer bonds are connected together to make a hairpin turn.

For a square lattice, which has a coordination number $q = 4$, there are $2N$ lattice bonds, provided we neglect the surface corrections. Let N_σ denote the number of square cells in state σ. The total number of cells is N; we neglect surface effects. We use "v" to denote the solvent (or voids) henceforth. Let N_M, N_E, N_v, and $N_m \equiv N - N_v$ denote the number of sites that are occupied by the middle groups, end groups, solvent species, and all the monomers, respectively. Then we have

$$N_M + N_E + N_v \equiv N \tag{2.1}$$

To take the thermodynamic limit, we let $N \to \infty$, so that N_M, N_E, and N_v diverge, but the corresponding densities $\phi_M = N_M/N$, $\phi_E = N_E/N$, and $\phi_v = N_v/N$ ($\phi_m \equiv 1 - \phi_v$) remain fix. Thus, eq 2.1 can be written in terms of densities as follows:

$$\phi_M + \phi_E + \phi_v \equiv 1 \tag{2.2}$$

Let B and p denote the total number of chemical bonds in all polymers and the total number of polymer chains, respectively. If N_{vv}, N_{EE}, N_{MM}, N_{Mv}, N_{Ev}, and N_{ME} denote the number of unbonded contacts between solvent−solvent, end group/end group, middle group/middle group, middle group/solvent, end group/solvent, and middle group/end group pairs, respectively, then it is easy to verify the following topological identities:

$$\begin{gathered}
N = N_0 + N_1 + N_g + N_p + N_h \\
2B = N_1 + 2(N_g + N_p) + 3N_h \\
4N_v = 2N_{vv} + N_{Mv} + N_{Ev} \\
4N_M = 2(B - p) + 2N_{MM} + N_{Mv} + N_{ME} \\
4N_E = 2p + 2N_{EE} + N_{ME} + N_{Ev} \\
2p = N_E \\
2(N_{MM} + N_{vv} + N_{EE} + N_{Mv} + N_{Ev} + N_{ME}) = 4N_0 + \\
3N_1 + 2(N_g + N_p) + N_h
\end{gathered} \tag{2.3}$$

From eqs 2.1 and 2.3, it is easily seen that the following identity

$$2N = B + N_{Mv} + N_{Ev} + N_{ME} + N_{MM} + N_{EE} + N_{vv} \tag{2.4}$$

is satisfied, as expected. The lattice size N is kept fixed in the definition of the model partition function (see eq 2.7). We have 16 quantities (in addition to N), among which there are eight constraints (see eqs 2.1 and 2.3). Thus, there are eight independent quantities whose choice is a matter of convenience only; the physics will remain independent of the choice. We choose the following eight independent quantities to describe every state in our model: N_E, N_M, N_g, N_p, N_h, N_{Mv}, N_{Ev}, and N_{ME}. Corresponding to each of these independent quantities there exists a chemical potential or an interaction energy, which controls its number. As mentioned earlier, there is a three-site bending penalty $\epsilon > 0$ for each of the two possible gauche (g) bonds at each site of the lattice. There is no penalty for a trans bond. There is a four-site interaction of energy $\epsilon' > 0$ for each pair of neighboring parallel bonds. For the hairpin turn, we have a third energy of interaction $\epsilon'' > 0$ (ϵ'' is the energy of a hairpin turn over and above $2\epsilon + \epsilon'$). For each of the unbonded contacts N_{ij}, $i \neq j =$ M, E, v, there exists an exchange energy of interaction ϵ_{ij}. The total energy of the system is given by

$$\begin{aligned}
E &= \epsilon N_g + \epsilon' N_p + \epsilon'' N_h + \sum_{i \neq j = M,E,v} \epsilon_{ij} N_{ij} \\
&= \epsilon(N_g + aN_p + bN_h + c_{Mv}N_{Mv} + c_{ME}N_{ME} + c_{Ev}N_{Ev})
\end{aligned} \tag{2.5}$$

where we have introduced dimensionless ratios $a = \epsilon'/\epsilon$, $b = \epsilon''/\epsilon$, $c_{Mv} = \epsilon_{Mv}/\epsilon$, $c_{ME} = \epsilon_{ME}/\epsilon$, and $c_{Ev} = \epsilon_{Ev}/\epsilon$. It should be noted that the exchange energies could be expressed in terms of bare van der Waals energies e_{ij} as follows:

$$\epsilon_{ij} \equiv e_{ij} - (e_{ii} + e_{jj})/2, \quad i,j = \mathrm{M}, \mathrm{E}, \mathrm{v} \qquad (2.6)$$

We also introduce Boltzmann weights or activities, which control the density of the above states, as follows: $w = \exp(-\beta\epsilon)$, $w' = w^a$, $w'' = w^b$, and $w_{ij} = w^{c_{ij}}$, $i \neq j = \mathrm{M}, \mathrm{E}, \mathrm{v}$, for the gauche bonds, parallel bonds, hairpin turn, and middle group/solvent, middle group/end group, and end group/solvent pairs, respectively. Here, $\beta = 1/\tilde{T}$ is the inverse temperature, and $\tilde{T}$ is measured in the units of the Boltzmann constant. We introduce a dimensionless temperature $T = \tilde{T}/\epsilon$, which will be used throughout the paper to measure the temperature. The densities of the end groups and the middle groups and their fluctuations are controlled by the activities $H = w^{-\mu_\mathrm{E}}$ and $\eta_\mathrm{M} = w^{-\mu_\mathrm{M}}$, respectively, where μ_E and μ_M play the role of the respective reduced (dimensionless) chemical potentials, normalized by ϵ. The presence of the activity H ensures that the polymer number is not fixed. The partition function for fixed N is given by

$$Z_N = \sum \eta_\mathrm{M}^{N_\mathrm{M}} H^{2p} w^{N_\mathrm{g}} w'^{N_\mathrm{p}} w''^{N_\mathrm{h}} \prod_{ij} w_{ij}^{N_{ij}} \qquad (2.7)$$

where the sum is over all distinct states, as characterized by the eight independent quantities. Each polymer has two end groups. Hence, $p \equiv N_\mathrm{E}/2$ represents the number of polymers in a given configuration. In addition, B represents the total number of chemical bonds in them. We do not allow middle group or end group monomers to exist by themselves. Thus, we are considering the properties of the polymers at 100% conversion. The smallest polymer has no middle group.

It should be pointed out that neither the number of bonds in each polymer nor their number is fixed in the average state. Thus, polymers appearing in eq 2.7 are polydisperse. The free energy per site $z_0 = (1/N) \ln Z_N$ in the limit $N \to \infty$ is the adimensional osmotic pressure $Pv_0/\tilde{T}$ across a membrane through which the solvent can pass through without any penalty, as shown elsewhere.[55] Here, P is the conventional osmotic pressure and v_0 the lattice cell volume. However, the reduced (dimensionless) osmotic pressure $P_\mathrm{r} \equiv Pv_0/\epsilon$ is a convenient quantity and plays a useful role in our investigation. If the solvent is replaced by voids, then the osmotic pressure becomes the pressure. As $\eta_\mathrm{M} \to \infty$, and $H \to 0^+$ or $p = 1$, the model reduces to the Hamilton walk limit problem studied earlier.[19,20] In particular, the model reduces to the Hamilton walk problem at absolute zero, provided $\mu_\mathrm{M} > 0$ and $\mu_\mathrm{E} < 0$; however, it only contains finite polymers at any positive temperature.

It is important to understand the nature of some of the interactions in our model. We first observe that physical interactions can only occur between material species, which are the monomers (middle and end groups) and the solvent in our model. These interactions can be either isotropic or anisotropic (orientation dependent). Both these interactions can also be interchain and intrachain. In our model, the isotropic interactions are described by the excess energy of interactions ϵ_{ij}. However, to create an ordered state, these interactions are not sufficient, and anisotropic interactions have to be incorporated in the model. These interactions are in addition to ϵ_{ij}. Let us consider the bending penalty $\epsilon > 0$, which represents one of the intrachain interactions requiring three consecutive monomers along a chain. Its positive value ensures that the polymers will become stiff at low temperatures. A negative value of ϵ will not result in stiff polymers at low temperatures and does not have to be considered. Thus, the choice of the sign of ϵ is dictated by the ability of the model to describe real systems. Its value can be determined by fitting the predictions of the calculation with experiments, which rules out a negative ϵ for polymers that crystallize at low temperatures. Other intrachain interactions relate to hairpin turns.

The parallel bond energy ϵ' in our model represents both intra- and interchain interactions and has been used earlier (see, for example, ref 15a). Our interaction should be distinguished from a purely interchain parallel bond interaction that has been used in other contexts, such as in ref 24b. (However, in the extreme limit $\epsilon \to \infty$, our parallel bond interaction also represents a purely interchain interaction.) In the absence of any bending penalty ($\epsilon = 0$), a negative ϵ' is required for a crystalline phase. When both interactions are present, there is a competition between them, as discussed in detail in refs 19 and 20. It has been shown there that $a < 1$ for the crystalline phase (parallel bonds) to occur at low temperatures.

Note. The requirement $\epsilon' > 0$ (repulsive parallel bond interaction) for a first-order melting does not imply that our model is not appropriate for real polymers. Appropriate parameters for each real system can be obtained by fitting the results of the model with experimental data as said above. Note that ϵ' is the interaction between two adjacent parallel "bonds". This interaction does not include the interaction between the four monomers that form the two bonds or, for that matter, any other interaction. The attractive interaction for parallel packing of rigid-rod-like chains usually referred to in the literature not only represents the interchain interaction but also includes the isotropic interaction between the rods (or monomers); hence, the two quantities are different and should not be compared. To the best of our knowledge, the exact quantity ϵ' as defined here has not been obtained experimentally; hence, in our opinion, the sign of ϵ' could only be determined by matching the predictions of our theory with experiments.

Finally, we note that at least two other papers, refs 15a and 24b, have discussed the need for a repulsive parallel bond interaction to obtain a first-order melting in equilibrium polymerization systems. We refer the reader to these references for further details.

As discussed in refs 19−21, and also mentioned above, we only consider $a < 1$ here, for which the ground state at $T = 0$ is the one in which all bonds are parallel ($N_\mathrm{p} = N$) with no bends ($N_\mathrm{g} = 0$) (see 1 and 2 in Figure 3). This is a completely ordered crystalline state. [For $a > 1$, the ground state is a steplike walk, see 3 and 4 in Figure 3, with maximum number of bends ($N_\mathrm{g} = N$), but no neighboring parallel bonds ($N_\mathrm{p} = 0$).[19−21] This state does not correspond to a crystal.] In the incompressible model with the Hamilton walk limit,[19,20] the appropriate range for a (with $b = 0$) was identified as between 0 and 1 by considering the ground state and the requirement for a first-order melting. For $a < 0$ (attractive parallel bond energy ϵ') and $b = 0$, the melting turns into a continuous transition.[19−21] (In the present model, too, the range for the parameters will be restricted by similar requirements.)

III. Husimi Lattice Theory

As the model cannot be solved exactly on a square lattice, we resort to some approximate calculation. We

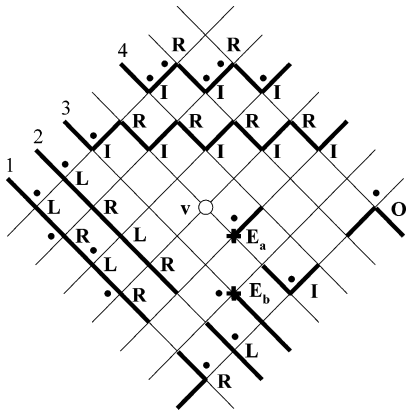

Figure 3. Seven states at a site and the possible ground states. The end groups are denoted by a cross (×) and the solvent or void by an empty circle (○); the remaining sites are covered by the middle groups. The filled dots (●) denote the corner of Σ, with Σ′ across it. We show the sequence of dots for configurations 1 and 4 of the walk.

make one approximation: we replace the square lattice by a Husimi cactus (see Figure 1). As discussed in detail in ref 20, the cactus represents the checkerboard version of the square lattice, in which we consider only the red squares or the black squares, as there are only two squares Σ and Σ′ (across from each other) that meet at each site in the cactus as opposed to four squares in the square lattice; compare Figures 1 and 3. (Even on a square lattice, however, there are only two squares across from each other.) Despite the difference, the coordination number is the same in both lattices. We then solve the model exactly on the cactus. The exact solution becomes an approximate theory on the square lattice.

The cactus is an infinitely large tree, obtained by joining two squares at each corner recursively. It is divided into generations, such that the generation number m at each site increases as we move away from the origin of the cactus, denoted by $m = 0$. Each square of the cactus has four sites: one at the base, which is close to the origin, one at the peak, and two intermediate sites. We index the base site by m, the two intermediate sites with $(m + 1)$, and the peak site with $(m + 2)$, as shown in Figure 1.

In our model, there are seven distinct possible states at each site, as described below. Each site on the cactus is shared by two squares Σ and Σ′ (see refs 19 and 20); Σ is marked by the filled dot close to the site, as shown in Figure 3. We must consider the checkerboard version of the square lattice shown in Figure 3. Consider some Σ and the site near the filled dot. This site identifies the companion square Σ′. To define six of the seven states, we proceed as follows. From inside Σ, we look across the shared site into the opposite square Σ′. The six states L, R, O, I, E_b, and E_a correspond to a left turn, a right turn, an outside turn in Σ′, an internal turn in Σ, and an end group at the site connected to a polymer coming from below or above that site, respectively. The last state is the one where the site is occupied by a solvent molecule; such a state is denoted by v.

We define partial partition functions (PPF's) $Z_m(\alpha)$ at the mth generation site given that the state at the site is α = L, R, I, O, v, E_b, and E_a; $Z_m(\alpha)$ is the contribution from the part of the cactus above the mth site and is expressed in the form of recursion relations (RR's) in terms of the partial partition functions at higher sites with indices $(m + 1)$ and $(m + 2)$ within the square. Thus, the RR's for the PPF's can be symbolically written[52] as $Z_m(\alpha) = J_\alpha[\{Z_{m+1}(\alpha')\}, \{Z_{m+2}(\alpha'')\}]$, where J_α is a cubic polynomial in all of its arguments, but a quadratic polynomial in the two arguments $Z_{m+1}(\alpha')$. We introduce the seven ratios

$$x_m(\alpha) = Z_m(\alpha)/[Z_m(\mathrm{L}) + Z_m(\mathrm{R})]$$

for α = L, R, I, O, v, E_b, and E_a, and

$$x_m(\mathrm{R}) = 1 - x_m(\mathrm{L})$$

The RR's for $Z_m(\alpha)$ yield the RR's for $x_m(\alpha)$. On an infinite cactus, the RR's for $x_m(\alpha)$ will approach a fixpoint (FP) solution near the origin. The FP solution describes the thermodynamics of the homogeneous bulk system. In case there are several FP solutions, then the most stable solution will determine the homogeneous bulk behavior in the model. As discussed earlier,[19−21] we will consider two different schemes for the FP to identify the amorphous and crystalline phases.

Construction of Recursion Relations. As an example, we show here how the PPF for state I (see section A of the Appendix) is obtained. We need to consider all possible distinct configurations of the square, with level m (the bottom vertex) in state I, as shown in Figure 4. The statistical weight of each configuration of the square is given in section C of the Appendix, and Z_m(I) is the obtained by summing these weights. Let us show how the statistical weight of the configuration shown in Figure 4i is obtained. The two intermediate $(m + 1)$ levels are in state R and O; the peak $(m + 2)$ level is in state E_b. Thus, the contribution from these states in Figure 4i is $Z_{m+1}(\mathrm{R})Z_{m+1}(\mathrm{O})Z_{m+2}(E_b)$. In addition, we have to account for the two gauche bonds, a pair of parallel bonds, a hairpin turn, the interaction between the end group and the middle group within the square, and the presence of the middle group at level m. The additional multiplicative contribution is $\eta_M w^2 w' w'' w_{ME}$. We do not have to include an activity η_M for the middle groups at the $(m + 1)$ levels, or an activity H for the end group at the $(m + 2)$ level, because those activities will be included in the corresponding PPF at levels $(m + 1)$ or $(m + 2)$. Therefore, the total statistical weight from the configuration in Figure 4i is $\eta_M w^2 w' w'' w_{ME} Z_{m+1}(\mathrm{R})Z_{m+1}(\mathrm{O})Z_{m+2}(E_b)$, as shown in section C of the Appendix. The statistical weights of other configurations in Figure 4 are obtained in a similar fashion. The recursion relations for states α = O, v, L, E_a, and E_b are obtained similarly by considering all the distinct configurations of the square with level m in state α. We only show the configurations for state I as the numbers of distinct configurations for other states are very large.

We present the recursion relations, the expression for z_0, calculation of various densities, and the average degree of polymerization (M) in section A of the Appendix.

Amorphous Phase: One-Cycle FP Scheme. For the amorphous phase, the FP solution is very simple. As we approach the origin, $x_m(\alpha) \to x_\alpha$, regardless of the index m. We set $x_\alpha = l, i, o, s, e_b$, and e_a, for α = L, I, O, v, E_b, and E_a, respectively, and $x_R \equiv r = 1 - l$. In the amorphous phase, due to symmetry, $Z_m(\mathrm{L}) = Z_m(\mathrm{R})$, we always have $l = r = 1/2$.

Crystal Phase: Two-Cycle FP Scheme. The role of the two-cycle solution has been explained earlier.[19−21] In this cycle pattern, the lattice has a sublattice

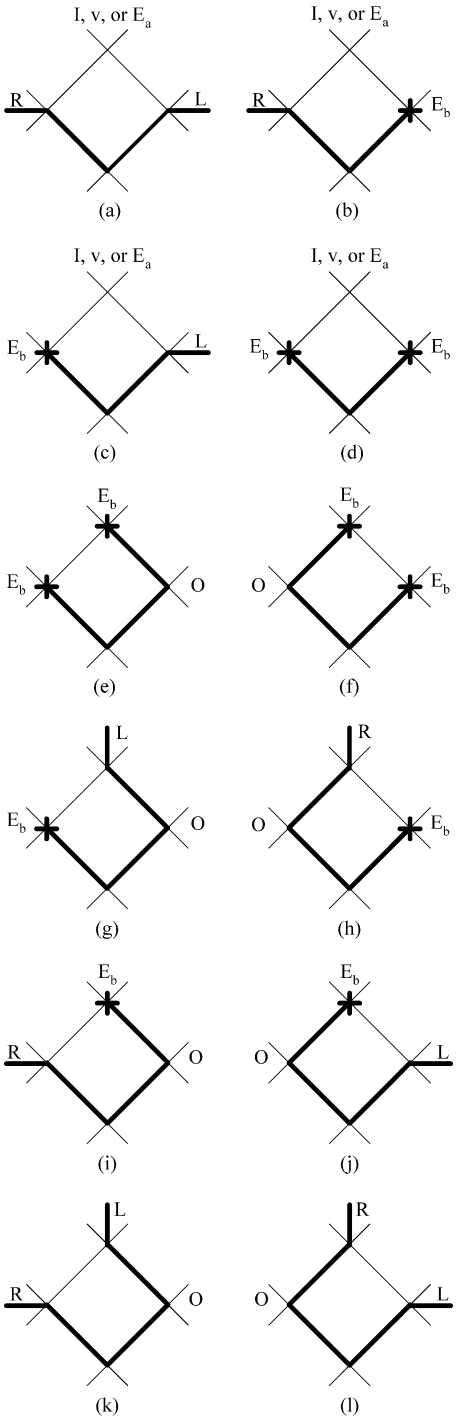

Figure 4. Distinct configurations of the square with the level m in state I. The statistical weight of each configuration is given in section C of the Appendix.

structure: the sites along any chosen direction alternate between two types A and B. Thus, l or r on each sublattice A or B will no longer be $^1/_2$. However, if $l > {}^1/_2$ on sublattice A (or B), then $r > {}^1/_2$ on sublattice B (or A), and the pattern repeats itself. The relation $l + r = 1$ is still valid on each sublattice. At $T = 0$, the crystal (CR) has $l_A = 1$, $l_B = 0$ or vice versa. The phase separation will always be present in real systems, which have a repulsive monomer−solvent interaction ($c_{Mv} > 0$ and $c_{Ev} > 0$). If the solvent is athermal, there is no phase separation, even at $T = 0$. We do not consider this athermal case, as it is not realistic. The free energy per site is calculated by considering the possible states at the origin using the Gujrati trick.[52] The methodology of this calculation is presented in ref 20 and will not be reported here.

IV. Results and Discussion

Before we present our results, we briefly discuss the appropriate choice of parameters. As said earlier, we take $0 < a < 1$. The energy barrier for the trans ↔ gauche rotation in polyethylene has been estimated[56] to be between 2.5 and 6.4 kJ/mol. The barrier to rotation of course depends on the nature of bonds, side groups, etc., that are specific to each species; however, we will use the energy barrier for polyethylene here taking it as a representative value. If we consider the solvent to represent the free volume, the exchange energy $\epsilon_{Mv} = -e_{MM}/2$, where e_{MM} is the bare van der Waals energy of interaction between the middle groups. A good estimate for $-e_{MM}$ appears to be in the range 0.1−1.8 kcal/mol[57] (assuming that the coordination number in the bulk is ≅10). Therefore, rough estimates indicate that the appropriate values for c_{Mv} are between 0.03 and 1.5. However, if the solvent represents a material species and not the free volume, ϵ_{Mv} will be much smaller and the higher limit on the choice of c_{Mv} will be much smaller; it may be close to zero. Similar arguments apply to the choice of c_{Ev}. The ratio c_{ME}, however, will usually be small as ϵ_{ME} is the exchange energy between two material species and will usually be small. In most of the calculations, we fix the reduced (osmotic) pressure $P_r \cong 1$, as we get reasonable values for the solvent/free volume density in the liquid and the crystal for this pressure. The cell volume v_0 is often used as a fitting parameter,[58] specific to a given system; therefore, extracting the pressure P from the value of P_r is system-dependent. In the figures, we do not show the dimension because all those quantities are dimensionless. Both the energy (E) and the latent heat per monomer (L_m) are normalized by ϵ.

We allow for variable concentration of end groups through its activity H, which is what is expected under condition of equilibrium polymerization. The absence of free monomers (100% conversion) should not be a concern since our goal is not to study the polymerization process itself but to study the melting properties of the final (polydisperse) polymer system with model parameters. The polydispersity gives rise to an average degree of polymerization (DP) that can be controlled by varying various parameters in the theory. For example, letting $H \to 0$, we can make the average DP $M \to \infty$.

The observed behavior in the model is very rich because of the number of parameters. Therefore, we only present selective results here to demonstrate this richness. It is hoped that this will suffice to convince the reader that novel features emerge due to the interplay of various parameters.

1. Middle Group Interaction. We first study how the properties at the melting point change with the middle group/solvent interaction (c_{Mv}). This interaction is the most important one as most of the polymer chain is composed of middle groups. This interaction also defines the solvent quality. As c_{Mv} increases, the solvent gradually becomes a more poor solvent. Thus, our discussion on the effect of c_{Mv} is also useful to provide information on the effect of solvent quality on the melting properties. In Figure 5a we fix the pressure $P_r = 1$ and show how the melting temperature (T_M) and the latent heat per monomer (L_m) change with c_{Mv}.

We find that with increasing c_{Mv} T_M increases monotonically. The direct relation between the strength of

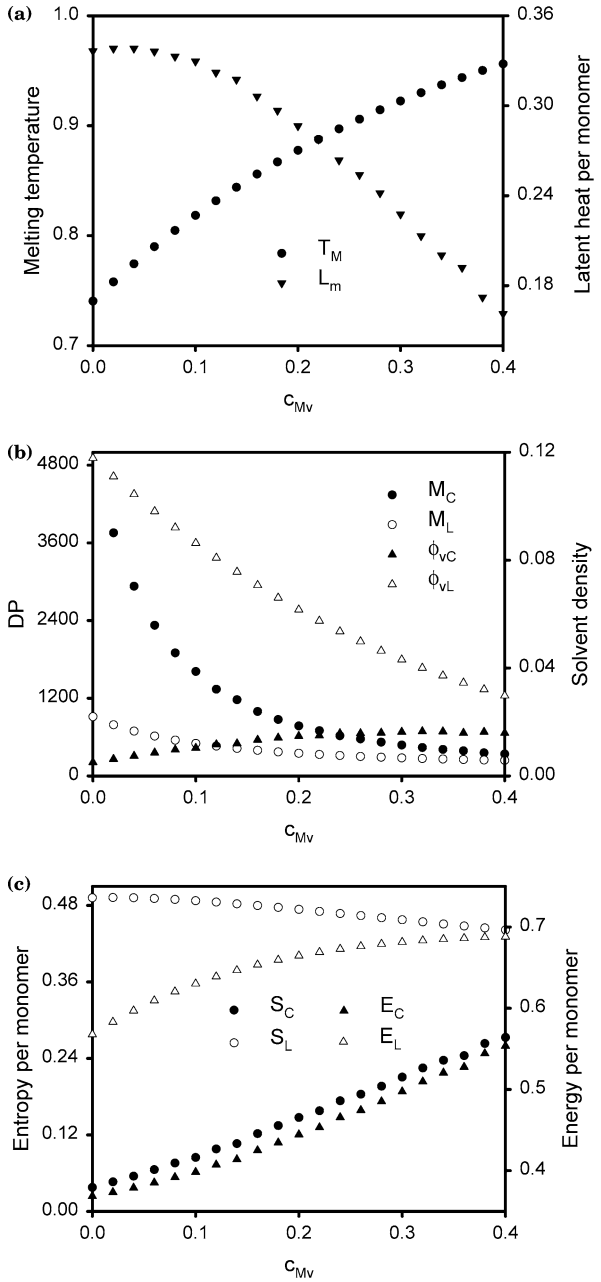

Figure 5. Effect of c_{Mv} at fixed reduced pressure $P_r = 1$ on (a) the melting temperature and the latent heat per monomer, (b) degree of polymerization and solvent density in the crystal and liquid at the melting point, and (c) entropy and energy per monomer in the crystal and liquid. The other parameters are fixed as follows: $a = 0.7$, $c_{ME} = 0.01$, $c_{Ev} = 0.04$, $\mu_E = -5$, and $b = 0$.

monomer interactions and the melting temperature in the case of fixed length polymers has been established from experimental data for a number of systems by Bunn.[57] The results presented here for the polydisperse case supplement these classic results.

We have found that as c_{Mv} increases, the melting gradually becomes continuous and then remains continuous. This can also be inferred from Figure 5a–c. Continuous melting refers to the transition from an amorphous phase to an ordered phase or vice versa in a continuous fashion as the system variable is changed. For example in Figure 5, we change c_{Mv} and study the properties at the melting point. When c_{Mv} is larger than some value, the amorphous phase smoothly turns into the ordered phase, without any discontinuity in any of the thermodynamic quantities such as the density of the monomers, gauche bonds, etc. There is also no latent heat of melting, which implies that there is no discontinuity in the energy and entropy of the two phases. In fact, at this stage, there is no "discontinuous melting point". From Figure 5b,c, as discussed later, we find that as c_{Mv} is increased, M, free volume density, S (entropy), and E (energy) in the crystal and liquid phase approach each other (i.e., the difference between them decreases). Thus, we can infer that as c_{Mv} is increased, the difference between the thermodynamic variables in the crystal and liquid at the melting point decreases, and at a sufficiently high value of c_{Mv} the difference will become zero, implying that "melting" is now "continuous". Continuous melting is also referred to as second-order transition. This contrasts to first-order melting, where a discontinuity in the thermodynamic variables exists at the melting point.

In our model, the crystal only has liquid crystalline ordering and does not contain any point-group symmetry of a conventional crystal. Hence, the melting in our model can be continuous. Indeed, Menon and Pandit[15b] have used Monte Carlo simulation on a square lattice, which has the same coordination number and the smallest square loops as the Husimi cactus, to verify that the melting in the Flory model is continuous. In the following, we will only consider cases where melting is first order. It is obvious that accounting for intermolecular interactions with the correct values is important to yield a first-order melting. This is also consistent with our earlier observation.[19,20] A similar result was also obtained by Nagle[4] for the dimer model for polyethylene, where the melting is continuous for very strong intermolecular attractive interactions and becomes first order when the interactions are reduced to the physical range. All these observations are inconsistent with Flory's hypothesis[2] that intermolecular interactions do not play an important role in melting. The observations are also at odds with the conclusions drawn in ref 10a. Consistent with our findings, however, Bunn[57] has argued that the energy barrier to rotation is of the same order of magnitude as the intermolecular interactions, and hence both intermolecular interactions and molecular flexibility are equally important in determining the melting point and other properties.

In Figure 5b, we show how M and ϕ_v in the crystal (CR) and the equilibrium liquid (EL) at the melting point change with c_{Mv}. We notice that the degree of polymerization of CR (M_C) is always larger than the degree of polymerization of EL (M_L). Such a discontinuity in the degree of polymerization has been observed in theoretical results[23–25] and Monte Carlo simulations[13,15] of equilibrium polymerization, although the latter calculations have been performed at fixed monomer chemical potential rather than fixed pressure. The CR free volume ϕ_{vC} is smaller than the EL free volume ϕ_{vL}. With increasing c_{Mv}, we find that both M_C and M_L decrease, with the drop in M_C being much larger. The CR free volume increases while ϕ_{vL} decreases with increasing c_{Mv}, with the change in ϕ_{vL} being much larger. At $c_{Mv} = 0.4$, the difference between M_C and M_L, and between ϕ_{vC} and ϕ_{vL}, is about 100 and 0.01, respectively.

In Figure 5c, we show the entropy and energy per monomer in CR (S_C and E_C) and EL (S_L and E_L) at the melting point for various c_{Mv}. We find that with increasing c_{Mv} both E_C and E_L monotonically increase, albeit

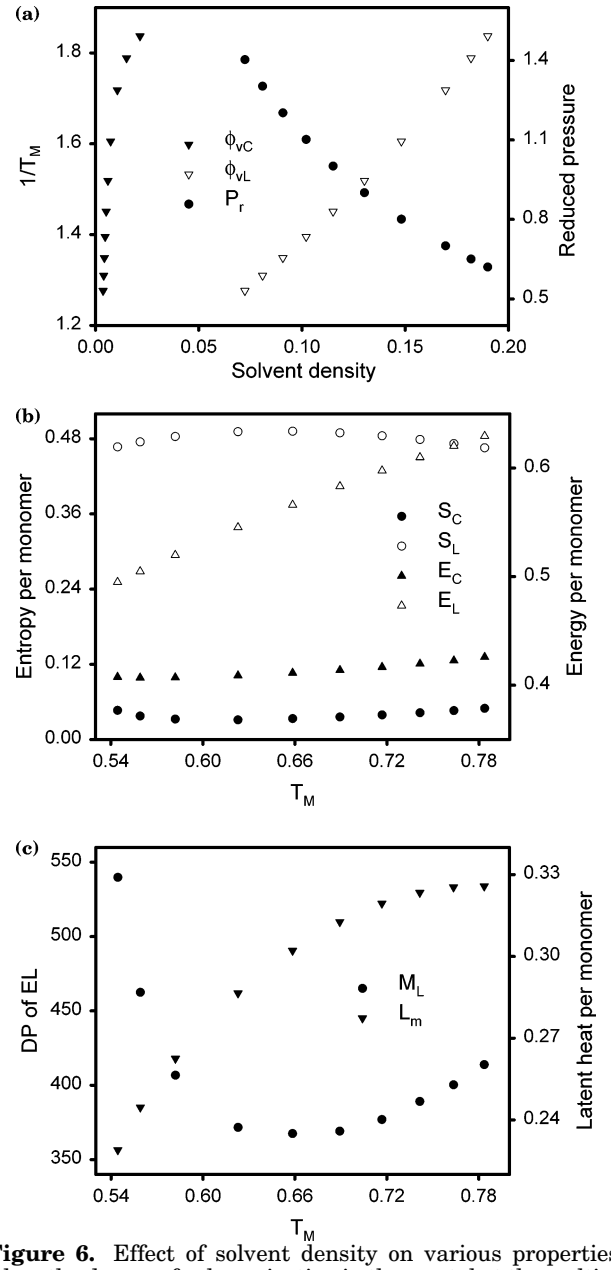

Figure 6. Effect of solvent density on various properties, when the degree of polymerization in the crystal at the melting point is fixed at 2000. (a) The inverse melting temperature with the solvent density in crystal and liquid. We also show the reduced pressure at the melting point as a function of the solvent density in the liquid. (b) Entropy and energy per monomer in the crystal and liquid with the melting temperature corresponding to different pressures at the melting point. (c) The degree of polymerization in the liquid and the latent heat per monomer with the melting temperature. The other parameters are fixed as follows: $a = 0.8$, $c_{Mv} = 0.01$, $c_{Ev} = 0.01$, $c_{ME} = 0.01$, and $b = 0$.

with opposite curvatures. With increasing c_{Mv}, S_C increases dramatically, while S_L decreases slightly. Thus, with increasing c_{Mv}, the difference in S_C and S_L continuously decreases and the melting temperature increases (see Figure 5a). However, latent heat per monomer L_m goes through a maximum at $c_{Mv} \cong 0.03$ and then decreases with increasing c_{Mv}, when the drop in the entropy of melting exceeds the rise in the melting temperature.

2. Solvent (or Free Volume) Density. We now study the effect of solvent (or free volume) on properties at the melting point. To provide a reference for comparison, we fix $M_C = 2000$ at the melting point; the rest of the parameters are as shown in Figure 6. Flory[1] has obtained the following relation for the depression of the melting temperature due to the presence of low degree of polymerization diluents that is applicable to both polydisperse (these are not same as equilibrium polymerization considered here) and fixed length polymers:

$$1/T_M - 1/T_M^0 = \epsilon[\phi_{vL} + (\phi_{mL} + \lambda)/M_L - \delta\phi_{vL}^2]/h_u \quad (4.1)$$

where the notation has been modified slightly (recall that our temperature is scaled by ϵ, which explains its presence above). Here M_L is the average DP in EL and $\phi_{mL} = 1 - \phi_{vL}$. For large M_L and small ϕ_{vL}, λ may be taken as a constant. The enthalpy of fusion per structural unit is h_u, δ is related to the cohesive energy density, and T_M^0 is the melting temperature of an infinite length polymer in the absence of diluents. Using eq 4.1 as a basis for our study, in Figure 6a, we plot the solvent density in CR and in EL at the melting point against the inverse melting temperature. In Figure 6a, we also show the reduced pressure at the melting point as a function of ϕ_{vL}. The reduced pressure behaves as we expect: it increases as both ϕ_{vL}, and the corresponding ϕ_{vC} decrease. Note: In Figure 6a, we have plotted the reduced pressure independently of $1/T_M$. In the figure, the largest reduced pressure corresponds to the smallest value of $1/T_M$ and vice versa.

In Figure 6b, we show how S_C, S_L, E_C, and E_L change with the melting temperature. We find that S_C, S_L, and E_C are almost constant, but E_L increases somewhat linearly with T_M. In Figure 6c, we show M_L and L_m at the melting point (M_C fixed at 2000). We find that with increasing T_M L_m increases and reaches its asymptotic value at higher T_M, where the pressure is also higher; however, M_L goes through a minimum.

3. DP *M*. The first expression for the effect of DP on the equilibrium melting temperature was derived by Flory[1] by treating the end groups as a different species with independent contributions to the free energy. In the absence of any diluent, a linear relation between the inverse melting temperature and the inverse average degree of polymerization was found.

We fix the pressure $P_r = 1$ at the melting point and plot $1/T_M$ against $1/M_C$ and $1/M_L$ in Figure 7a. We do not distinguish between the end groups and the middle groups ($c_{ME} = 0$, $c_{Mv} = c_{Ev} = 0.01$) in this case; the rest of the parameters are as shown. In Figure 7b, we show S_C, S_L, E_C, and E_L at the melting point against M_L. We find that both S_C and S_L decrease with increasing M_L and quickly achieve asymptotic values. The difference between S_C and S_L also stabilizes, and this causes L_m to stabilize at high DP, as we see in Figure 7c.

With increasing M_L, E_L increases while E_C decreases, but both achieve asymptotic values at high DP. In Figure 7c, we show ϕ_{vC}, ϕ_{vL}, and L_m against M_L. We find that ϕ_{vL} increases slightly but is almost constant. On the other hand, ϕ_{vC} decreases with increasing M_L and appears to go to zero or remain very small for high DP.

A unique feature of our theory is that the end group interactions can be incorporated. We have investigated the effect of having attractive middle group and end group interactions ($c_{ME} < 0$). We will only discuss our results here without presenting them, as the end group effect is weak. For $c_{ME} < 0$, ϕ_{vC} increases and ϕ_{vL} decreases; thus, the discontinuity in the free volume also decreases. Similarly, the discontinuities in the average DP, the entropy, and the energy per monomer also

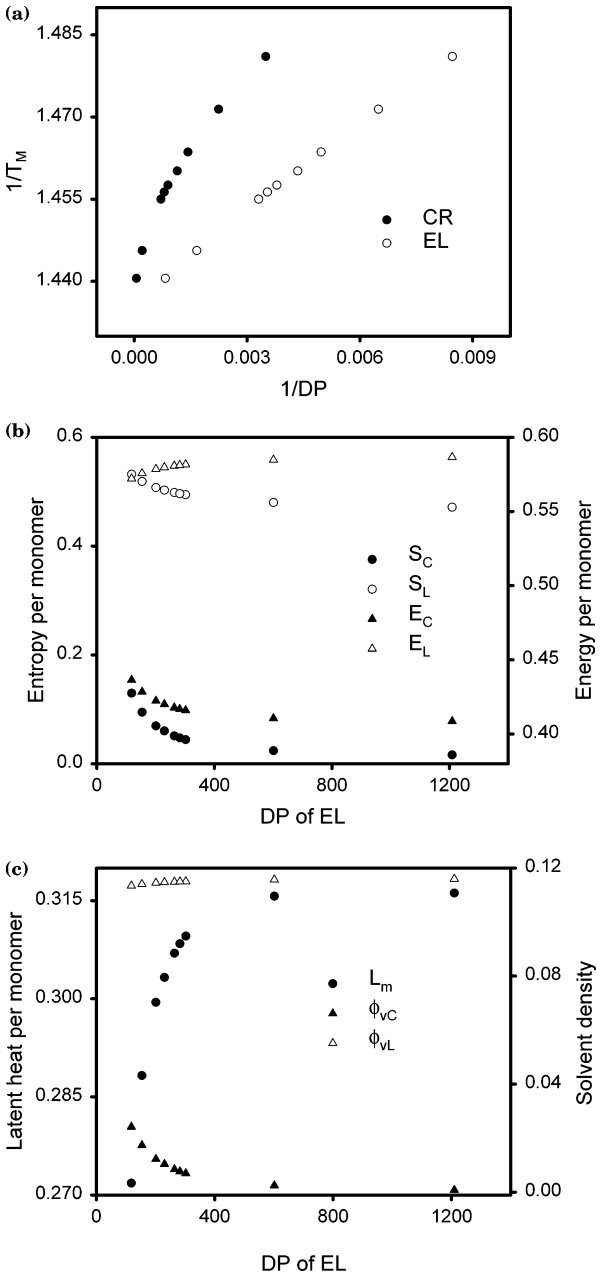

Figure 7. Effect of degree of polymerization on various properties for fixed pressure $P_r = 1$ at the melting point. (a) The inverse melting temperature, with the inverse degree of polymerization of the liquid and the crystal. (b) Entropy and energy per monomer in the crystal and the liquid with the degree of polymerization of the liquid at the melting point. (c) The solvent density in the crystal and liquid, and the latent heat per monomer with the degree of polymerization of the liquid. The other parameters are fixed as follows: $a = 0.8$, $c_{Mv} = 0.01$, $c_{ME} = 0$, $c_{Ev} = 0.01$, and $b = 0$.

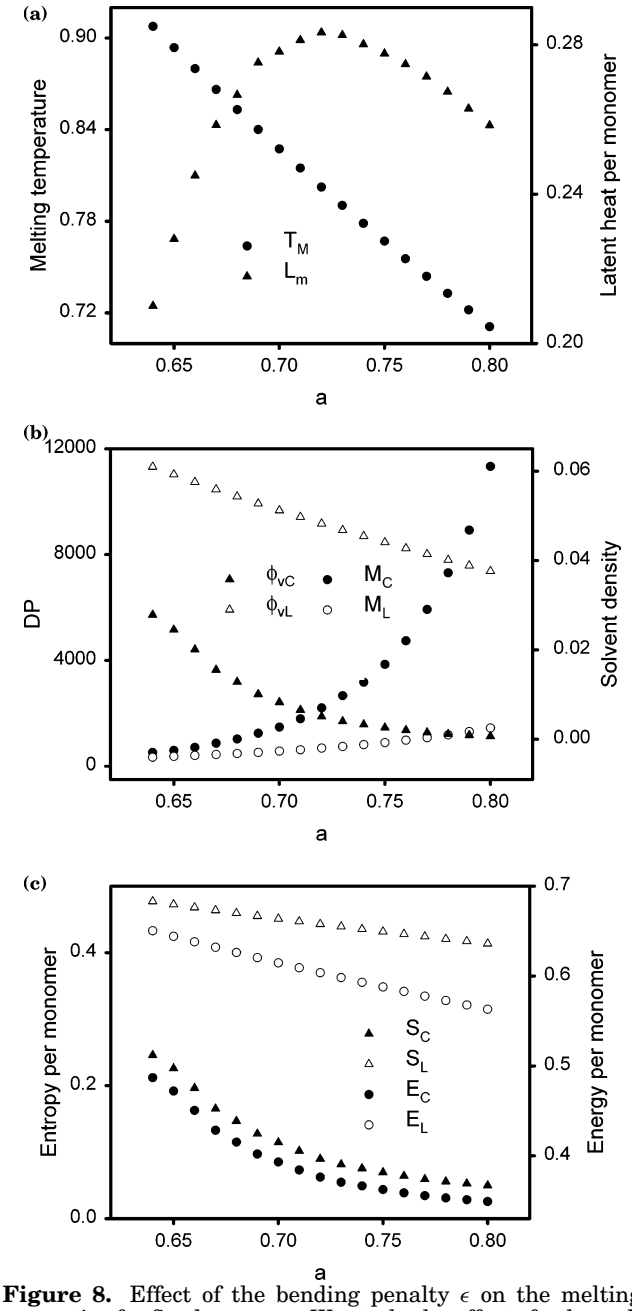

Figure 8. Effect of the bending penalty ϵ on the melting properties for fixed pressure. We study the effect of ϵ through $a = \epsilon'/\epsilon$, by keeping ϵ' fixed. The melting temperature T_M, the energies E_C and E_L, and the latent heat per monomer L_m are normalized by ϵ_0, which is the value of ϵ when $a = 0.64$. When $a = 0.64$, the other parameters are $c_{Mv} = 0.2$, $c_{ME} = 0.01$, $c_{Ev} = 0.3$, $b = 0$, $\mu_E = -5$, and $P_r = 1$. When $a \neq 0.64$, these parameters are recalculated with the new ϵ such that w_{Mv}, w_{ME}, w_{Ev}, w'', H (at any given $\tilde{T}$), and the pressure P are unchanged. We show (a) melting temperature and latent heat per monomer. (b) Degree of polymerization and solvent density in the crystal and liquid. (c) Entropy and energy per monomer in the crystal and liquid at the melting point.

decrease. The effect on T_M is too small to be discernible, while the latent heat per monomer slightly decreases. All these effects vanish for higher degree of polymerizations.

4. Chain Rigidity. In the classical theory of Flory,[2] chain rigidity is determined by a single parameter, the bending penalty ϵ. A similar definition for the chain rigidity has also been used by other authors.[4,57,59] In our theory, however, there are three energy parameters ϵ, ϵ', and ϵ'' that all determine chain rigidity. If we reduce ϵ', the number of pairs of neighboring parallel bonds N_p will increase, which can be considered as a sign of higher chain rigidity. If ϵ is increased, trans bonds will be favored, and this can also be considered as increasing the chain rigidity. To maximize N_p and minimize N_g, we would like to have smaller N_h, which will require a larger ϵ''. Thus, chain rigidity in our theory can be manipulated in more than one way, and we will consider the effects of ϵ, ϵ', and ϵ'' separately to gain a better understanding of the effect of chain rigidity.

(i) Effect of ϵ. In Figure 8, we consider the effect of ϵ on the melting properties by considering values of a between 0.64 and 0.8. Since the temperature T, the

reduced pressure, and the ratios a, b, c_{Mv}, c_{Ev}, and c_{ME} are all normalized by ϵ, care must be exercised in studying the effect of ϵ. Therefore, at the starting value, when $a = 0.64$, we take $c_{Mv} = 0.2$, $c_{ME} = 0.01$, $c_{Ev} = 0.3$, $b = 0$, $\mu_E = -5$, and $P_r = 1$. Let ϵ_0 denote the value of ϵ when $a = 0.64$. When we consider any other value of a, the values of c_{Mv}, c_{ME}, c_{Ev}, b, μ_E, and P_r are recalculated with the new ϵ so that w_{Mv}, w_{ME}, w_{Ev}, w'', and H at any given unscaled temperature $\tilde{T}$ (recall that $\tilde{T}$ is not scaled by ϵ) and the normal pressure P are unchanged. This method ensures that only ϵ is changing, while other quantities and the normal pressure are kept fixed.

In Figure 8a, we show how T_M and L_m change with ϵ. As there are different values of ϵ for different choices of a, it will be difficult to compare the results if we report T_M which are normalized with different values of ϵ. Therefore, we have normalized the temperature T by ϵ_0 everywhere when calculating T_M on the y-axis. We find that T_M decreases linearly with decreasing ϵ (increasing a). The latent heat per monomer L_m is also now normalized by ϵ_0 everywhere. It goes through a maximum and then decreases rapidly with increasing ϵ. For small a (and when $b = 0$), the melting becomes continuous as evident from Figure 8b,c.

In Figure 8b, we show how M_C, M_L, ϕ_{vC}, and ϕ_{vL} change with ϵ. We find that the change in M_L with ϵ is much smaller than the change in M_C. With increasing ϵ, M_C continuously decreases until the melting becomes continuous for some $a < 0.64$. At $a = 0.64$ the difference between M_C and M_L is $\cong$200. The solvent density in CR increases with increasing ϵ to $\cong$3% for $a = 0.64$. These results on the changes in the solvent density with ϵ are qualitatively consistent with those obtained by Flory for fixed length polymers.[2]

In Figure 8c, we show how S_C, S_L, E_C, and E_L change with ϵ at the melting point. Again, in this figure, the energies E_C and E_L are normalized by ϵ_0 everywhere for ease of comparison. We find that S_C, S_L, E_C, and E_L all increase with increasing ϵ. However, S_C and E_C increase more rapidly than their counterparts in EL.

(ii) Effect of ϵ'. We have also investigated the effect of changing ϵ' alone while keeping other parameters fixed. The results are shown in Figure 9, where we have taken the range of a between 0.64 and 0.88 but kept c_{Mv}, c_{ME}, c_{Ev}, b, μ_E, and $P_r = 1$ fixed for all a. From Figure 9a, we find that T_M increases linearly, while L_m goes through a maximum and then decreases with decreasing ϵ'. From Figure 9b,c, we again find that the melting becomes continuous for small a (when $b = 0$).

(iii) Effect of ϵ''. Gujrati et al.[5–8] have shown that the hairpin turn excitations are important at low temperatures as they disorder the ground state. If these defects are suppressed, we expect the melting temperature to increase. In Figure 10a, we show how T_M and L_m vary with b for $P_r = 1$. We find that when b is increased slightly above zero, both T_M and L_m increase with b. In Figure 10b, we show the density of gauche bonds (ϕ_g) in CR and EL with b. We find that when b is increased slightly above zero, ϕ_g in both CR and EL decrease; however, the difference is almost constant. The jump in ϕ_g to higher values in going from CR to EL has also been studied by simulations.[13–15]

We note that decreasing ϵ', increasing ϵ, and increasing ϵ'' all of which are related to the notion of increasing chain rigidity in our model have conflicting effects on the melting properties, such as S_C, S_L, E_C, E_L, and L_m, as can be clearly seen from Figures 8−10. For example,

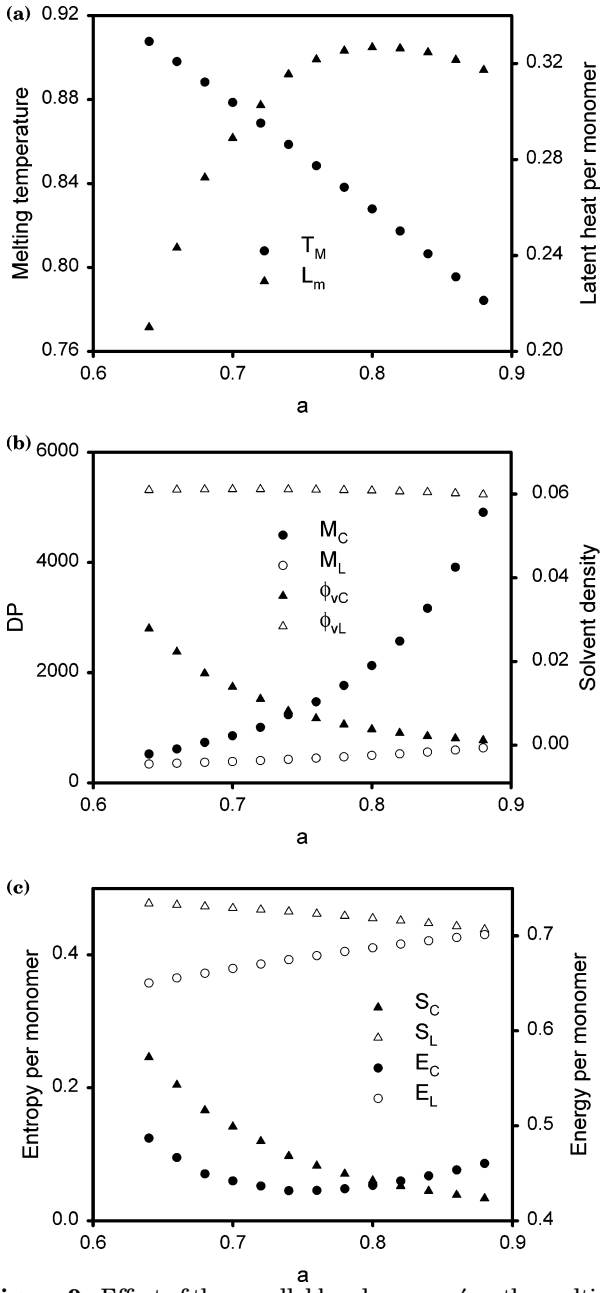

Figure 9. Effect of the parallel bond energy ϵ' on the melting properties for fixed pressure $P_r = 1$. The other parameters are fixed as follows: $c_{Mv} = 0.2$, $c_{ME} = 0.01$, $c_{Ev} = 0.3$, $b = 0$, and $\mu_E = -5$. We show (a) melting temperature and latent heat per monomer. (b) Degree of polymerization and solvent density in the crystal and liquid. (c) Entropy and energy per monomer in the crystal and liquid at the melting point.

from Figure 8c, we find that increasing ϵ leads to increase in the values of E_L; however, from Figure 9c, we find that decreasing ϵ' leads to a decrease in the value of E_L. Another example is that in Figure 8c; we find that with increasing ϵ, E_C increases monotonically. However, in Figure 9c, when ϵ' is decreased, E_C goes through a minimum instead of rising monotonically. Thus, the different measures of chain rigidity may have competing effects on the melting properties, and to properly characterize the effect of chain rigidity, we will need to know the values of ϵ, ϵ', and ϵ''.

V. Discussion and Conclusions

We have considered a general model for crystallization under equilibrium polymerization in a solution. The

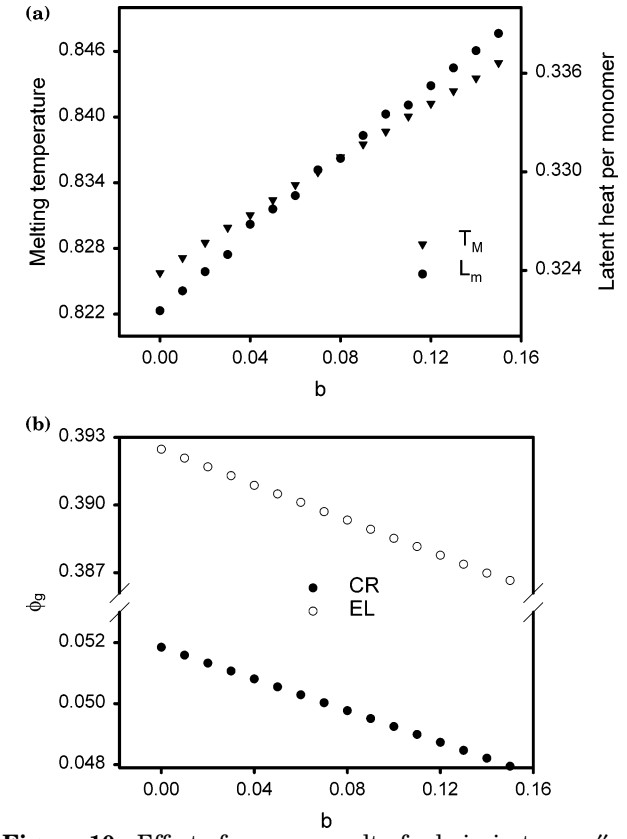

Figure 10. Effect of energy penalty for hairpin turns ϵ'' on the melting properties for fixed pressure $P_r = 1$. The other parameters are fixed as follows: $a = 0.8$, $c_{Mv} = 0.2$, $c_{ME} = -0.05$, $c_{Ev} = 0.1$, and $\mu_E = -5$. We show (a) melting temperature and latent heat per monomer. (b) Density of gauche bonds in the crystal and the liquid.

chains have variable polydispersity, whose nature is affected by the parameters and the temperature in the system in a specific manner, determined by equilibrium thermodynamics. The model is solved on a Husimi cactus using recursion techniques. The CR phase is identified with a two-cycle FP solution of the recursion relations, while the disordered equilibrium phase EL is identified with a one-cycle solution. The Husimi cactus solution of the model is taken to be an approximate theory on the square or the tetrahedral lattice. The theory is thermodynamically consistent in the entire parameter space and provides a first principle basis to study polymers formed under conditions of equilibrium polymerization.

We wish to point out the improvement our Husimi cactus solution provides, as discussed in ref 52 also, over the classical Flory–Huggins theory of melting by comparing the predictions of our solution with Monte Carlo simulations carried out by Menon and Pandit[15a] on a square lattice, which has the same coordination number q as the cactus. The simulations on a square lattice clearly show that the melting transition is continuous and belongs to the Ising universality class for $a < 0$. This is consistent with our results on the cactus but in disagreement with the predictions of the classical theory for $q = 4$, the coordination number that is suitable for a tetrahedral lattice. Therefore, it should come as no surprise that we have taken $a > 0$ in our calculation.

We should also point out that our statistical mechanical calculation describes equilibrium properties. In particular, our crystals refer to equilibrium crystals that are homogeneous. In this sense, our calculation does not describe metastable states such as a mixed state containing crystalline and amorphous regions. Such a state doers not have the lowest free energy because of the presence of interfaces. The equilibrium state corresponds to a homogeneous phase in which the chemical potentials are constant throughout the volume, whereas a mixed state will not satisfy this homogeneity of phase and chemical potential constancy requirements.

Our results clearly establish that there is only one melting transition in our model as we change the temperature, keeping the pressure and the chemical potential μ_E fixed. This is consistent with our earlier suggestion that this polydisperse system is similar to a monodisperse system. The crystal is the equilibrium state at and below and the disordered liquid at and above the melting temperature T_M. There is no equilibrium liquid that could further freeze into another crystal below T_M. Thus, having a sequence of freezing transitions at different temperatures at a constant P in the $T-P$ plane is not possible. This behavior should be contrasted with what may happen in system B, in which a crystal can precipitate out, leaving behind an equilibrium liquid that can again show precipitation of another crystal of a different molecular weight at a lower temperature and so on because of the multicomponent nature of system B.

In summary, the crystallization under equilibrium polymerization is studied with model parameters to evaluate the effects of chain rigidity, monomer interactions, solvent quality and quantity, degree of polymerization, energy penalty for bends, parallel bonds, and hairpin turns (which are important at low temperatures) on properties such as the melting temperature, latent heat, and energy and entropy of fusion. We find that the different measures of chain rigidity in our model may have competing effects on the melting properties, and therefore, care must be exercised in characterizing the effect of chain rigidity. To the best of our knowledge, such an explicit study of the relation between the melting properties in equilibrium polymerization and molecular parameters has not been conducted elsewhere. Our theory, which is also mean field, goes beyond the mean field approach of the Flory theory of melting, and hence, we believe our results will further the research in this area.

Acknowledgment. We thank Andrea Corsi for various discussions.

Appendix

We shall use the following short-hand notation for simplicity:

$$X(\alpha) \equiv Z_m(\alpha),\ Y(\alpha) \equiv Z_{m+1}(\alpha),\ Z(\alpha) \equiv Z_{m+2}(\alpha),\ u \equiv w_{ME},\ z \equiv w_{Ev},\ \text{and}\ y \equiv w_{Mv}$$

A. Crystalline Phase: Two-Cycle Scheme. The PPF's $Z_m(L)$ and $Z_m(R)$ can be broken into contributions from trans and gauche states. Therefore, we have

$$X(L) = X(L_t) + X(L_g),\quad X(R) = X(R_t) + X(R_g)$$

Owing to the symmetry of L and R states, we also have the following identities:

$$X(R_t) = X(L_g)/w,\quad X(R_g) = wX(L_t)$$

We obtain the following seven independent recursion relations:

$$X(L_t) = \eta_M[uZ(I)Y(I)Y(E_b) + uy^2Y(E_b)Y(v)Z(I) + zyY(E_b)Z(v)[Y(I) + Y(v)] + u^3Y(E_b)Z(I)Y(E_a) + z^2uY(E_b)Z(v)Y(E_a) + uY(E_b)Y(I)Z(E_a) + zyY(E_b)Y(v)Z(E_a) + uZ(E_a)Y(E_a)Y(E_b) + Z(I)Y(I)Y(R) + y^2Y(v)Z(I)Y(R) + y^2Z(v)Y(I)Y(R) + y^2Z(v)Y(v)Y(R) + u^2Y(E_a)Z(I)Y(R) + yzuZ(v)Y(E_a)Y(R) + u^2Z(E_a)Y(I)Y(R) + uzyZ(E_a)Y(v)Y(R) + u^2Z(E_a)Y(E_a)Y(R) + u^2w'Y^2(E_b)Z(L) + w'Z(E_b)Y(E_b)Y(R) + 2uw'Y(E_b)Z(L)Y(R) + uw'Z(E_b)Y^2(E_b) + uw'Z(E_b)Y^2(R) + w'Z(L)Y^2(R) + u^2w'Z(E_b)Y(E_b)Y(R) + wZ(R)Y(O)Y(I) + wy^2Y(O)Y(v)Z(R) + wu^2Y(E_a)Y(O)Z(R) + wuZ(E_b)Y(O)Y(I) + wzyZ(E_b)Y(v)Y(O) + wuY(E_a)Z(E_b)Y(O) + w''w^2w'Z(O)Y(O)[uY(E_b) + Y(R)]]$$

$$X(L_g) = \eta_M[w[uZ(I)Y(I)Y(E_b) + uy^2Y(E_b)Y(v)Z(I) + zyY(E_b)Z(v)[Y(I) + Y(v)] + u^3Y(E_b)Y(E_a)Z(I) + z^2uY(E_b)Y(E_a)Z(v) + uY(E_b)Y(I)Z(E_a) + zyY(E_b)Y(v)Z(E_a) + uY(E_b)Y(E_a)Z(E_a)] + wY(L)[Y(I)Z(I) + y^2Y(v)Z(I) + y^2Y(I)Z(v) + y^2Z(v)Y(v) + u^2Z(I)Y(E_a) + yzuZ(v)Y(E_a) + u^2Z(E_a)Y(I) + uzyZ(E_a)Y(v) + u^2Z(E_a)Y(E_a)] + w[u^2w'Y^2(E_b)Z(R) + w'Z(E_b)Y(E_b)Y(L) + uw'Z(R)Y(L)Y(E_b) + uw'Z(E_b)Y^2(E_b) + uw'Z(R)Y(E_b)Y(L) + uw'Z(E_b)Y^2(L) + w'Z(R)Y^2(L) + u^2w'Z(E_b)Y(E_b)Y(L)] + w[wZ(L)Y(O)Y(I) + wy^2Z(L)Y(v)Y(O) + wu^2Z(L)Y(E_a)Y(O) + wuZ(E_b)Y(O)Y(I) + wzyZ(E_b)Y(O)Y(v) + wuZ(E_b)Y(E_a)Y(O) + w''w^2w'Z(O)Y(O)[uY(E_b) + Y(L)]]]$$

$$X(v) = Z(v)Y^2(v) + 2z^2Z(v)Y(v)Y(E_a) + z^2Y^2(v)Z(E_a) + 2y^2Z(v)Y(v)Y(I) + y^2Y^2(v)Z(I) + 2z^2Y(v)Y(E_a)Z(E_a) + 2uyzZ(E_a)Y(v)Y(I) + 2uzyY(E_a)Y(v)Z(I) + 2y^2Y(v)Y(I)Z(I) + z^4Z(v)Y^2(E_a) + 2z^2y^2Y(E_a)Z(v)Y(I) + y^4Z(v)Y^2(I) + yzY(v)Y(E_b)[Z(R) + Z(L)] + yzY(v)Z(E_b)[Y(L) + Y(R)] + y^2Y(v)[Z(R)Y(L) + Y(R)Z(L)] + 2z^2Y(v)Y(E_b)Z(E_b) + z^2Y^2(E_a)Z(E_a) + 2uzyZ(E_a)Y(E_a)Y(I) + u^2z^2Y^2(E_a)Z(I) + 2uzyZ(I)Y(I)Y(E_a) + u^2y^2Z(E_a)Y^2(I) + y^2Z(I)Y^2(I) + z^2uY(E_b)Y(E_a)[Z(R) + Z(L)] + zyY(E_b)Y(I)[Z(R) + Z(L)] + yzZ(E_b)Y(E_a)[Y(L) + Y(R)] + uy^2Z(E_b)Y(I)[Y(L) + Y(R)] + uzyY(E_a)[Z(R)Y(L) + Y(R)Z(L)] + y^2Y(I)[Z(R)Y(L) + Y(R)Z(L)] + 2z^2Z(E_b)Y(E_b)Y(E_a) + 2uzyZ(E_b)Y(E_b)Y(I) + y^2wZ(O)Y(L)Y(R) + z^2wY^2(E_b)Z(O) + zywZ(O)Y(E_b)[Y(L) + Y(R)]$$

$$X(E_b) = H[Z(E_a)Y^2(E_a) + 2Z(E_b)Y(E_b)Y(E_a) + 2z^2Y(v)Y(E_a)Z(E_a) + z^2Z(v)Y^2(E_a) + 2u^2Y(E_a)Y(I)Z(E_a) + u^2Y^2(E_a)Z(I) + 2z^2Y(v)Z(E_b)Y(E_b) + 2u^2Z(E_b)Y(E_b)Y(I) + uY(E_b)Y(E_a)[Z(R) + Z(L)] + uZ(E_b)Y(E_a)[Y(L) + Y(R)] + wY^2(E_b)Z(O) + 2z^2Y(E_a)Y(v)Z(v) + 2zyuY(E_a)[Z(v)Y(I) + Y(v)Z(I)] + 2u^2Y(E_a)Y(I)Z(I) + z^4Z(E_a)Y^2(v) + 2z^2u^2Y(v)Z(E_a)Y(I) + u^4Z(E_a)Y^2(I) + uY(I)Y(E_b)[Z(R) + Z(L)] + zyY(E_b)Y(v)[Z(R) + Z(L)] + u^3Y(I)Z(E_b)[Y(L) + Y(R)] + z^2uZ(E_b)Y(v)[Y(L) + Y(R)] + u^2Y(E_a)[Y(L)Z(R) + Z(L)Y(R)] + wuY(E_b)Z(O)[Y(R) + Y(L)] + u^2Z(I)Y^2(I) + 2uzyY(v)Y(I)Z(I) + z^2u^2Z(v)Y^2(I) + 2zuyZ(v)Y(v)Y(I) + z^2y^2Y^2(v)Z(I) + z^2Z(v)Y^2(v) + u^2Y(I)[Y(L)Z(R) + Z(L)Y(R)] + yzuY(v)[Y(L)Z(R) + Z(L)Y(R)] + u^2wY(L)Y(R)Z(O)]$$

$$X(O) = \eta_M[Z(I)Y^2(I) + 2y^2Z(I)Y(I)Y(v) + y^2Y^2(I)Z(v) + 2u^2Z(I)Y(I)Y(E_a) + u^2Y^2(I)Z(E_a) + 2yzuY(I)Y(v)Z(E_a) + 2yzuY(I)Z(v)Y(E_a) + 2y^2u^2Z(I)Y(E_a)Y(v) + 2y^2Z(v)Y(v)Y(I) + 2u^2Y(I)Y(E_a)Z(E_a) + y^4Y^2(v)Z(I) + u^4Z(I)Y^2(E_a) + Y(I)[Z(L)Y(R) + Y(L)Z(R)] + uY(I)[Y(E_b)Z(L) + Y(R)Z(E_b) + Y(L)Z(E_b) + Y(E_b)Z(R)] + 2u^2Y(I)Y(E_b)Z(E_b) + y^2Y^2(v)Z(v) + 2yzuY(E_a)Y(v)Z(v) + y^2z^2Y^2(v)Z(E_a) + 2yzuY(v)Y(E_a)Z(E_a) + z^2u^2Y^2(E_a)Z(v) + u^2Y^2(E_a)Z(E_a) + u^3Z(L)Y(E_b)Y(E_a) + y^2uY(v)Y(E_b)Z(L) + u^3Z(R)Y(E_a)Y(E_b) + y^2uY(v)Y(E_b)Z(R) + uY(R)Z(E_b)Y(E_a) + yzY(v)Z(E_b)[Y(R) + Y(L)] + uY(L)Z(E_b)Y(E_a) + u^2Y(E_a)[Z(L)Y(R) + Y(L)Z(R)] + y^2Y(v)[Z(L)Y(R) + Y(L)Z(R)] + 2u^2Z(E_b)Y(E_b)Y(E_a) + 2yzuZ(E_b)Y(E_b)Y(v) + wY(L)Y(R)Z(O) + wuY(E_b)Z(O)[Y(L) + Y(R)] + wu^2Y^2(E_b)Z(O)]$$

$$X(I) = \eta_M[wY(L)Y(R)Z(I)] + wy^2Y(L)Y(R)Z(v) + wu^2Y(L)Y(R)Z(E_a) + wuY(E_b)Z(I)[Y(R) + Y(L)] + wzyY(E_b)Z(v)[Y(R) + Y(L)] + wuY(E_b)Z(E_a)[Y(R) + Y(L)] + wu^2Z(I)Y^2(E_b) + wz^2Z(v)Y^2(E_b) + wZ(E_a)Y^2(E_b) + w''w^2w'[2Y(O)Y(E_b)Z(E_b) + uY(O)Y(E_b)[Z(R) + Z(L)] + uY(O)Z(E_b)[Y(R) + Y(L)] + Y(O)[Y(R)Z(L) + Z(R)Y(L)]]]$$

$$X(\mathrm{E_a}) = H[2Z(\mathrm{E_a})Y(\mathrm{E_a})Y(\mathrm{E_b}) + 2w'Z(\mathrm{E_b})Y^2(\mathrm{E_b}) + 2z^2Y(\mathrm{E_b})Z(\mathrm{E_a})Y(\mathrm{v}) + 2u^2Z(\mathrm{E_a})Y(\mathrm{E_b})Y(\mathrm{I}) + 2z^2Y(\mathrm{E_a})Y(\mathrm{E_b})Z(\mathrm{v}) + 2u^2Y(\mathrm{E_b})Y(\mathrm{E_a})Z(\mathrm{I}) + uZ(\mathrm{E_a})Y(\mathrm{E_a})[Y(\mathrm{L}) + Y(\mathrm{R})] + w'uY^2(\mathrm{E_b})[Z(\mathrm{R}) + Z(\mathrm{L})] + 2w'uZ(_{\mathrm{b}})Y(\mathrm{E_b})[Y(\mathrm{L}) + Y(\mathrm{R})] + 2wZ(\mathrm{E_b})Y(\mathrm{E_a})Y(\mathrm{O}) + 2z^2Y(\mathrm{E_b})Y(\mathrm{v})Z(\mathrm{v}) + 2zyuY(\mathrm{E_b})[Z(\mathrm{I})Y(\mathrm{v}) + Y(\mathrm{I})Z(\mathrm{v})] + 2u^2Y(\mathrm{E_b})Y(\mathrm{I})Z(\mathrm{I}) + uY(\mathrm{E_a})Z(\mathrm{I})[Y(\mathrm{R}) + Y(\mathrm{L})] + zyY(\mathrm{E_a})Z(\mathrm{v})[Y(\mathrm{R}) + Y(\mathrm{L})] + u^3Z(\mathrm{E_a})Y(\mathrm{I})[Y(\mathrm{R}) + Y(\mathrm{L})] + z^2uZ(\mathrm{E_a})Y(\mathrm{v})[Y(\mathrm{R}) + Y(\mathrm{L})] + u^2w'Y(\mathrm{E_b})[Y(\mathrm{R})Z(\mathrm{L}) + Z(\mathrm{R})Y(\mathrm{L})] + w'Y(\mathrm{E_b})[Z(\mathrm{L})Y(\mathrm{R}) + Y(\mathrm{L})Z(\mathrm{R})] + w'u^2Z(\mathrm{E_b})[Y^2(\mathrm{R}) + Y^2(\mathrm{L})] + uwY(\mathrm{E_a})Y(\mathrm{O})[Z(\mathrm{L}) + Z(\mathrm{R})] + 2w^2w'w''Y(\mathrm{E_b})Y(\mathrm{O})Z(\mathrm{O}) + uZ(\mathrm{I})Y(\mathrm{I})[Y(\mathrm{R}) + Y(\mathrm{L})] + zyY(\mathrm{v})Z(\mathrm{I})[Y(\mathrm{R}) + Y(\mathrm{L})] + uy^2Z(\mathrm{v})Y(\mathrm{I})[Y(\mathrm{R}) + Y(\mathrm{L})] + zyZ(\mathrm{v})Y(\mathrm{v})[Y(\mathrm{R}) + Y(\mathrm{L})] + uw'[Z(\mathrm{L})Y^2(\mathrm{R}) + Z(\mathrm{R})Y^2(\mathrm{L})] + wuY(\mathrm{O})Y(\mathrm{I})[Z(\mathrm{R}) + Z(\mathrm{L})] + wzyY(\mathrm{v})Y(\mathrm{O})[Z(\mathrm{R}) + Z(\mathrm{L})] + w^2uw'w''Z(\mathrm{O})Y(\mathrm{O})[Y(\mathrm{R}) + Y(\mathrm{L})]]$$

The ratios l and r can be broken into contributions from trans and gauche states at the fixed point (in CR and EL):

$$l = l_{\mathrm{t}} + l_{\mathrm{g}}, \quad r = r_{\mathrm{t}} + r_{\mathrm{g}}$$

In CR, they have the following relationships: $r_{\mathrm{t}} = l_{\mathrm{g}}/w$, $r_{\mathrm{g}} = wl_{\mathrm{t}}$. We introduce the quantities Q_{LR} and Q_2, which are given by the relations

$$\Psi_m = {\Psi_{m+1}}^2\Psi_{m+2}Q_{\mathrm{LR}}, \quad Z = {\Psi_0}^2Q_2, \qquad \Psi_m \equiv Z_m(\mathrm{R}) + Z_m(\mathrm{L})$$

As there are two types of sites A and B, we obtain two expressions for Q_{LR} and Q_2. We present the equations for Q_{LR} and Q_2 below. For ease of writing, we denote the quantities evaluated on site A by a bar and those on site B with a hat. We get

$$\bar{Q}_2 = (2\bar{o}\bar{\imath} + {\bar{l}_{\mathrm{t}}}^2 + {\bar{r}_{\mathrm{t}}}^2 + 2\bar{r}_{\mathrm{g}}\bar{l}_{\mathrm{g}}/w)/\eta_{\mathrm{M}} + \bar{s}^2 + 2\bar{e}_a\bar{e}_b/H$$

$$\bar{Q}_{\mathrm{LR}} = \eta_{\mathrm{M}}(1+w)[u\bar{\imath}\hat{\imath}\hat{e}_b + uy^2\hat{e}_b\hat{s}\bar{\imath} + zy\hat{e}_b\bar{s}\hat{\imath} + zy\bar{s}\hat{s}\hat{e}_b + u^3\hat{e}_b\bar{\imath}\hat{e}_a + z^2u\hat{e}_b\bar{s}\hat{e}_a + u\hat{e}_b\hat{\imath}\bar{e}_a + zy\hat{e}_b\hat{s}\bar{e}_a + u\bar{e}_a\hat{e}_a\hat{e}_b + \bar{\imath}\hat{\imath}\hat{r} + y^2\hat{s}\bar{\imath}\hat{r} + y^2\bar{s}\hat{\imath}\hat{r} + y^2\bar{s}\hat{s}\hat{r} + u^2\hat{e}_a\bar{\imath}\hat{r} + yzu\bar{s}\hat{e}_a\hat{r} + u^2\bar{e}_a\hat{\imath}\hat{r} + uzy\bar{e}_a\hat{s}\hat{r} + u^2\bar{e}_a\hat{e}_a\hat{r} + u^2w'\hat{e}_b{}^2\bar{l} + w'\bar{e}_b\hat{e}_b\hat{r} + uw'\hat{e}_b\bar{l}\hat{r} + uw'\bar{e}_b\hat{e}_b{}^2 + uw'\hat{e}_b\bar{l}\hat{r} + uw'\bar{e}_b\hat{r}^2 + w'\bar{l}\hat{r}^2 + u^2w'\bar{e}_b\hat{e}_b\hat{r} + w\bar{r}\hat{o}\hat{\imath} + wy^2\hat{o}\hat{s}\bar{r} + wu^2\hat{e}_a\hat{o}\bar{r} + wu\bar{e}_b\hat{o}\hat{\imath} + wzy\bar{e}_b\hat{s}\hat{o} + wu\hat{e}_a\bar{e}_b\hat{o} + w^2w'u\bar{o}\hat{o}\hat{e}_b + w^2w'\bar{o}\hat{o}\hat{r} + u\bar{\imath}\hat{\imath}\hat{e}_b + uy^2\hat{e}_b\hat{s}\bar{\imath} + zy\hat{e}_b\bar{s}\hat{\imath} + zy\bar{s}\hat{s}\hat{e}_b + u^3\hat{e}_b\hat{e}_a\bar{\imath} + z^2u\hat{e}_b\hat{e}_a\bar{s} + u\hat{e}_b\hat{\imath}\bar{e}_a + zy\hat{e}_b\hat{s}\bar{e}_a + u\hat{e}_b\hat{e}_a\bar{e}_b + \hat{l}(\bar{\imath}\hat{\imath} + y^2\hat{s}\bar{\imath} + y^2\bar{s}\hat{\imath} + y^2\bar{s}\hat{s} + u^2\hat{e}_a\bar{\imath} + yzu\bar{s}\hat{e}_a + u^2\bar{e}_a\hat{\imath} + uzy\bar{e}_a\hat{s} + u^2\bar{e}_a\hat{e}_a) + u^2w'\hat{e}_b{}^2\bar{r} + w'\bar{e}_b\hat{e}_b\hat{l} + uw'\hat{e}_b\bar{r}\hat{l} + uw'\bar{e}_b\hat{e}_b{}^2 + uw'\hat{e}_b\hat{l}\bar{r} + uw'\bar{e}_b\hat{l}^2 + w'\bar{r}\hat{l}^2 + u^2w'\bar{e}_b\hat{e}_b\hat{l} + w\bar{l}\hat{o}\hat{\imath} + wy^2\hat{o}\hat{s}\bar{l} + wu^2\hat{e}_a\hat{o}\bar{l} + wu\bar{e}_b\hat{o}\hat{\imath} + wzy\bar{e}_b\hat{s}\hat{o} + wu\hat{e}_a\bar{e}_b\hat{o} + w^2w'u\bar{o}\hat{o}\hat{e}_b + w^2w'\bar{o}\hat{o}\hat{l}]$$

To obtain $\hat{Q}_2$ and $\hat{Q}_{\mathrm{LR}}$, we simply replace the bar and hat on i, o, s, r, l, e_a, and e_b in the above equations with a hat and bar, respectively.

The adimensional pressure

$$z_0 \equiv \beta P v_0 = 0.5\ln(\bar{Q}_{\mathrm{LR}}/\hat{Q}_2) = 0.5\ln(\hat{Q}_{\mathrm{LR}}/\bar{Q}_2)$$

Next we present the equations for various densities, which can be applied for both sites A and B. Use of either kind of site gives identical results. The density of the solvent, monomer, internal and external bends, end groups, left-trans, right-trans, left-gauche, right-gauche, left and right turns, and gauche bonds are given by

$$\phi_{\mathrm{v}} = \bar{s}^2/\bar{Q}_2,\ \phi_{\mathrm{m}} = 1 - \phi_{\mathrm{v}},\ \phi_{\mathrm{i}} = \phi_{\mathrm{o}} = 2\bar{o}\bar{\imath}/(\eta_{\mathrm{M}}\bar{Q}_2),\ \phi_{\mathrm{e}} = 2\bar{e}_a\bar{e}_b/(H\bar{Q}_2)$$

$$\phi_{l\mathrm{t}} = {\bar{l}_{\mathrm{t}}}^2/(\eta_{\mathrm{M}}\bar{Q}_2),\ \phi_{r_{\mathrm{t}}} = {\bar{r}_{\mathrm{t}}}^2/(\eta_{\mathrm{M}}\bar{Q}_2),\ \phi_{l_{\mathrm{g}}} = \phi_{r_{\mathrm{g}}} = \bar{r}_{\mathrm{g}}\bar{l}_{\mathrm{g}}/(w\eta_{\mathrm{M}}\bar{Q}_2),\ \phi_l = \phi_{l_{\mathrm{t}}} + \phi_{l_{\mathrm{g}}}$$

$$\phi_r = \phi_{r_{\mathrm{t}}} + \phi_{r_{\mathrm{g}}},\ \phi_{\mathrm{g}} = \phi_{\mathrm{i}} + \phi_{r_{\mathrm{g}}} + \phi_{l_{\mathrm{g}}}$$

The corresponding equations for site B (with a hat) can be obtained by replacing the bar with a hat above. The average degree of polymerization $M = \phi_{\mathrm{m}}/\phi_{\mathrm{p}}$, and the number density $\phi_{\mathrm{p}} = \phi_e/2$.

B. Amorphous Phase: One-Cycle Scheme. The recursion relations for the crystal also yield the solution for the amorphous phase when we set $Z(\alpha) \equiv Y(\alpha)$. In this case we also get other simple relations:

$$l_{\mathrm{t}} = 0.5/(1+w),\ l_{\mathrm{g}} = wl_{\mathrm{t}},\ r_{\mathrm{t}} = l_{\mathrm{t}},\ r_{\mathrm{g}} = l_{\mathrm{g}}$$

C. Statistical Weight of Each Configuration in Figure 4. (a) $\eta_{\mathrm{M}}wY(\mathrm{L})Y(\mathrm{R})Z(\mathrm{I})$ [for state I at $(m+2)$ level], $\eta_{\mathrm{M}}wy^2Y(\mathrm{L})Y(\mathrm{R})Z(\mathrm{v})$ [for state v at $(m+2)$ level], and $\eta_{\mathrm{M}}wu^2Y(\mathrm{L})Y(\mathrm{R})Z(\mathrm{E_a})$ [for state $\mathrm{E_a}$ at $(m+2)$ level]; (b) $\eta_{\mathrm{M}}wuY(\mathrm{E_b})Y(\mathrm{R})Z(\mathrm{I})$ [for state I at $(m+2)$ level], $\eta_{\mathrm{M}}wzyY(\mathrm{E_b})Y(\mathrm{R})Z(\mathrm{v})$ [for state v at $(m+2)$ level], and $\eta_{\mathrm{M}}wuY(\mathrm{E_b})Y(\mathrm{R})Z(\mathrm{E_a})$ [for state $\mathrm{E_a}$ at $(m+2)$ level]; (c) $\eta_{\mathrm{M}}wuY(\mathrm{E_b})Y(\mathrm{L})Z(\mathrm{I})$ [for state I at $(m+2)$ level], $\eta_{\mathrm{M}}wzyY(\mathrm{E_b})Y(\mathrm{L})Z(\mathrm{v})$ [for state v at $(m+2)$ level], and $\eta_{\mathrm{M}}wuY(\mathrm{E_b})Y(\mathrm{L})Z(\mathrm{E_a})$ [for state $\mathrm{E_a}$ at $(m+2)$ level]; (d) $\eta_{\mathrm{M}}wu^2Y^2(\mathrm{E_b})Z(\mathrm{I})$ [for state I at $(m+2)$ level], $\eta_{\mathrm{M}}wz^2Y^2(\mathrm{E_b})Z(\mathrm{v})$ [for state v at $(m+2)$ level], and $\eta_{\mathrm{M}}wY^2(\mathrm{E_b})Z(\mathrm{E_a})$ [for state $\mathrm{E_a}$ at $(m+2)$ level]; (e) $\eta_{\mathrm{M}}w^2w'w''Y(\mathrm{O})Y(\mathrm{E_b})Z(\mathrm{E_b})$; (f) $\eta_{\mathrm{M}}w^2w'w''Y(\mathrm{O})Y(\mathrm{E_b})Z(\mathrm{E_b})$; (g) $\eta_{\mathrm{M}}w^2w'w''uY(\mathrm{O})Y(\mathrm{E_b})Z(\mathrm{L})$; (h) $\eta_{\mathrm{M}}w^2w'w''uY(\mathrm{O})Y(\mathrm{E_b})Z(\mathrm{R})$; (i) $\eta_{\mathrm{M}}w^2w'w''uY(\mathrm{O})Y(\mathrm{R})Z(\mathrm{E_b})$; (j) $\eta_{\mathrm{M}}w^2w'w''uY(\mathrm{O})Y(\mathrm{L})Z(\mathrm{E_b})$; (k) $\eta_{\mathrm{M}}w^2w'w''Y(\mathrm{O})Y(\mathrm{R})Z(\mathrm{L})$; and (l) $\eta_{\mathrm{M}}w^2w'w''Y(\mathrm{O})Y(\mathrm{L})Z(\mathrm{R})$.

References and Notes

(1) Flory, P. J. *J. Chem. Phys.* **1942**, *10*, 51. (b) *J. Chem. Phys.* **1949**, *17*, 223. (c) Flory, P. J. *Trans. Faraday Soc.* **1955**, *51*, 848.
(2) Flory, P. J. *Proc. R. Soc. London, Ser. A* **1956**, *234*, 60. (b) *Proc. R. Soc. London, Ser. A* **1956**, *234*, 73.
(3) Flory, P. J.; Vrij, A. *J. Am. Chem. Soc.* **1963**, *85*, 3548.
(4) Nagle, J. F. *Proc. R. Soc. London, Ser. A* **1974**, *337*, 569.
(5) Gujrati, P. D. *J. Phys. A* **1980**, *13*, L437.
(6) Gujrati, P. D.; Goldstein, M. *J. Chem. Phys.* **1981**, *74*, 2596.
(7) Gujrati, P. D. *J. Stat. Phys.* **1982**, *28*, 241.

(8) Nagle, J. F.; Gujrati, P. D.; Goldstein, M. *J. Phys. Chem.* **1984**, *88*, 4599.
(9) Petschek, R. G. *Phys. Rev. B* **1985**, *32*, 474.
(10) Baumgartner, A.; Yoon, D. Y. *J. Chem. Phys.* **1983**, *79*, 521. (b) Baumgartner, A. *J. Chem. Phys.* **1986**, *84*, 1905.
(11) Saleur, H. *J. Phys. A* **1986**, *19*, 2409.
(12) Suzuki, J.; Izuyama, T. *J. Phys. Soc. Jpn.* **1988**, *57*, 818.
(13) Tuthill, G. F.; Jaric, M. V. *Phys. Rev. B* **1985**, *31*, 2981.
(14) Rouault, Y.; Milchev, A. *Phys. Rev. E* **1995**, *51*, 5905. (b) Milchev, A.; Landau, D. P. *Phys. Rev. E* **1995**, *52*, 6431.
(15) Menon, G. I.; Pandit, R. *Phys. Rev. E* **1999**, *59*, 787. (b) Chatterji, A.; Pandit, R. *Europhys. Lett.* **2001**, *54*, 213.
(16) Weber, H.; Paul, W.; Binder, K. *Phys. Rev. E* **1999**, *59*, 2168.
(17) Muthukumar, M. *Eur. Phys. J. E* **2000**, *3*, 199.
(18) Hu, W. *J. Chem. Phys.* **2000**, *113*, 3901.
(19) Gujrati, P. D.; Corsi, A. *Phys. Rev. Lett.* **2001**, *87*, 025701.
(20) Corsi, A.; Gujrati, P. D. *Phys. Rev. E* **2003**, *68*, 031502.
(21) Gujrati, P. D.; Rane, S. S.; Corsi, A. *Phys. Rev. E* **2003**, *67*, 052501.
(22) Pretti, M. *Phys. Rev. E* **2002**, *66*, 061802.
(23) Kindt, J. T.; Gelbart, W. M. *J. Chem. Phys.* **2001**, *114*, 1432.
(24) Briehl, R. W.; Herzfeld, J. *Proc. Natl. Acad. Sci. U.S.A.* **1979**, *76*, 2740. (b) Herzfeld, J.; Briehl, R. W. *Macromolecules* **1981**, *14*, 397. (c) Kramer, E. M.; Herzfeld, J. *Phys. Rev. E* **1998**, *58*, 5934.
(25) McMullen, W. E.; Gelbart, W. M.; Ben-Shaul, A. *J. Chem. Phys.* **1985**, *82*, 5616. (b) Odijk, T. *J. Phys*. (*Paris*) **1987**, *48*, 125. (c) van der Schoot, P.; Cates, M. E. *Langmuir* **1994**, *10*, 670. (d) van der Schoot, P.; Cates, M. E. *Europhys. Lett.* **1994**, *25*, 515.
(26) Gujrati, P. D. *Phys. Rev. B* **1989**, *40*, 5140. (b) See also eqs 37 and 38 and the discussion thereafter in: Gujrati, P. D. *Phys. Rev. B* **1987**, *35*, 8486.
(27) Greer, S. C. *Comput. Mater. Sci.* **1995**, *4*, 334. (b) Greer, S. C. *J. Phys. Chem.* **1998**, *102*, 5413.
(28) Cates, M. E. *J. Phys.: Condens. Matter* **1996**, *8*, 9167. (b) Cates, M. E.; Candau, S. J. *J. Phys.: Condens. Matter* **1990**, *2*, 6869.
(29) Wittmer, J. P.; Milchev, A.; Cates, M. E. *J. Chem. Phys.* **1998**, *109*, 834.
(30) Scott, R. L. *J. Phys. Chem.* **1965**, *69*, 261. (b) Anderson, E. M.; Greer, S. C. *J. Chem. Phys.* **1988**, *88*, 2666.
(31) Eisenberg, A.; Tobolsky, A. V. *J. Polym. Sci.* **1960**, *46*, 19.
(32) Tobolsky, A. V.; Eisenberg, A. *J. Am. Chem. Soc.* **1959**, *81*, 2302.
(33) Elias, H. G.; Fritz, A. *Makromol. Chem.* **1968**, *114*, 31.
(34) Oozawa, F.; Asakura. S. In *Thermodynamics in the Polymerization of Proteins*; Academic Press: New York, 1975. (b) Niranjan, P. S.; Forbes, J. G.; Greer, S. C.; Dudowicz, J.; Freed, K. F.; Douglas, J. F. *J. Chem. Phys.* **2001**, *114*, 10573.
(35) Wheeler, J. C.; Kennedy, S. J.; Pfeuty, P. *Phys. Rev. Lett.* **1980**, *45*, 1748. (b) Wheeler, J. C.; Pfeuty, P. *Phys. Rev. Lett.* **1981**, *46*, 1409. (c) Kennedy, S. J.; Wheeler, J. C. *J. Chem. Phys.* **1983**, *78*, 953.
(36) Gujrati, P. D. *Phys. Rev. A* **1981**, *24*, 2096. (b) Gujrati, P. D. *J. Phys. A* **1981**, *14*, L345. (c) Gujrati, P. D. *Phys. Rev. A* **1983**, *28*, 3589. (d) Gujrati, P. D. *Phys. Rev. B* **1983**, *27*, 4507.
(37) Gujrati, P. D. *Phys. Rev. A* **1988**, *38*, 5840.
(38) Gujrati, P. D. *Phys. Rev. Lett.* **1985**, *55*, 1161.
(39) Gujrati, P. D. *Phys. Rev. Lett.* **1984**, *53*, 2453.
(40) Gujrati, P. D. *Phys. Rev. B* **1989**, *40*, 5140.
(41) Gujrati, P. D. *Mod. Phys. Lett.* **1990**, *4*, 267. (b) Gujrati, P. D. *Int. J. Mod. Phys.* **1992**, *6*, 1193.
(42) Kaufman, M.; Berger, T.; Gujrati, P. D.; Bowman, D. *Phys. Rev. A* **1990**, *41*, 4371.
(43) Gujrati, P. D. *Phys. Lett. A* **1991**, *156*, 410.
(44) Gujrati, P. D. *J. Chem. Phys.* **1993**, *98*, 1613. (b) Gujrati, P. D. *Phys. Rev. E* **1995**, *51*, 957.
(45) Gujrati, P. D. *Phys. Rev. Lett.* **1995**, *74*, 1367.
(46) Erukhimovich, I. *JETP* **1995**, *81*, 553. (b) Erukhimovich, I.; Ermoshkin, A. V. *JETP* **1999**, *88*, 538. (c) Erukhimovich, I.; Ermoshkin, A. V. *J. Chem. Phys.* **2002**, *116*, 368.
(47) Semenov, A. N.; Nyrkova, I. A.; Cates, M. E. *Macromolecules* **1995**, *28*, 7879.
(48) Gujrati, P. D. *J. Chem. Phys.* **1998**, *108*, 5809.
(49) Semenov, A. N.; Rubinstein, M. *Macromolecules* **1998**, *31*, 1373.
(50) Gujrati, P. D.; Bowman, D. *J. Chem. Phys.* **1999**, *111*, 8151.
(51) Gujrati, P. D. *J. Phys. A* **2001**, *34*, 9211.
(52) Gujrati, P. D. *Phys. Rev. Lett.* **1995**, *74*, 809.
(53) Rane, S.; Gujrati, P. D. *Phys. Rev. E* **2001**, *64*, 011 801.
(54) Gujrati, P. D. *J. Phys. A: Math. Gen.* **2001**, *34*, 9211.
(55) Gujrati, P. D. *J. Chem. Phys.* **1998**, *108*, 6952.
(56) Robertson, M. B.; Klein, P. G.; Ward, I. M.; Packer, K. J. *Polymer* **2001**, *42*, 1261.
(57) Bunn, C. W. *J. Polym. Sci.* **1955**, *16*, 323.
(58) Rane, S. S.; Gujrati, P. D. *J. Chem. Phys.* **2002**, *116*, 3947.
(59) Foreman, K. W.; Freed, K. F. *J. Chem. Phys.* **1997**, *106*, 7422.

MA047622F